Industrial Chemistry & Materials

ROYAL SOCIETY OF CHEMISTRY

REVIEW

View Article Online
View Journal | View Issue

Cite this: *Ind. Chem. Mater.*, 2025, **3**, 681

Advances in coupling catalytic selective oxidation reactions with *in situ* synthesis of hydrogen peroxide

Jinghui Lyu, †* Han Wu,† Qingqing Li, Shihao Wang, Jinke Yao, Tao Liu, Wenying Chu, Feng Feng, Qunfeng Zhang, Qingtao Wang, Dahao Jiang, Guofu Zhang, Chunshan Lu, Chengrong Ding * and Xiaonian Li*

This review presents recent advances in coupling *in situ* hydrogen peroxide (H_2O_2) synthesis with selective oxidation reactions. As a green oxidant, H_2O_2 plays an important role in the chemical industry. However, conventional production methods often yield highly concentrated H_2O_2, which is not suitable for direct use in reactions and raises significant safety concerns. The integration of *in situ* H_2O_2 generation with selective oxidation allows for the immediate use of low-concentration H_2O_2, improving both safety and process efficiency. This review summarizes various strategies for *in situ* H_2O_2 production, including enzymatic and catalytic approaches, and discusses their application in representative oxidation reactions such as olefin epoxidation, benzene hydroxylation, methane oxidation, adipic acid synthesis, Fenton processes, oxidative desulfurization, and the oxidation of sulfides to sulfones. Special attention is given to recent developments in catalyst composition and structural design, particularly in olefin oxidation. This review concludes with a summary of the advantages of *in situ* H_2O_2 synthesis and offers perspectives on future research directions aimed at improving reaction efficiency, economic feasibility, and the development of sustainable green chemistry technologies.

Keywords: In situ hydrogen peroxide; Olefin epoxidation; Benzene hydroxylation; Tandem reaction; Desulfurization.

Received 16th June 2025,
Accepted 15th July 2025

DOI: 10.1039/d5im00103j

rsc.li/icm

1 Introduction

Hydrogen peroxide (H_2O_2), an essential inorganic chemical raw material and a primary green chemical, has been listed as one of the top essential 100 chemicals globally. It has a high content of reactive oxygen species (mass fraction is 47%), and the degradation by-product is only water, eliminating the separation and purification process after the reaction. It has become a substitute for oxidants such as *t*-BuOOH, HNO_3, N_2O, and permanganate commonly used in industries. H_2O_2 can be oxidized in a mild liquid environment, under acidic or alkaline conditions, compared with molecular oxygen. It is an efficient, strong multifunctional oxidant. Much research has been carried out to use H_2O_2 as the oxidant in the epoxidation of olefins, hydroxylation of aromatics, ammoxidation of ketones, and oxidation of alkanes. H_2O_2 has excellent industrial application prospects due to its advantages of high selectivity, mild reaction conditions, and green environmental protection.[1] The industrial method of producing H_2O_2 is mainly the anthraquinone method. The industrial technology of this method is mature, but there are some problems such as a large amount of equipment investment, complex process flow, and environmental pollution. Due to the limitation of process cost, H_2O_2 production plants are often built in remote areas, which need to be stored and transported to the point of use for dilution in industrial applications. However, high-concentration H_2O_2 is unstable, can easily decompose, has high storage and transportation cost, and has potential safety hazards. The direct synthesis of H_2O_2 from H_2 and O_2 has become a research hotspot because of its advantages of high atomic economy and good environmental benefits. Furthermore, there has been considerable focus on both electrocatalytic[2–4] and photocatalytic[5–7] pathways for synthesizing H_2O_2. It is

College of Chemical Engineering, State Key Laboratory of Green Chemical Synthesis and Conversion, Zhejiang Key Laboratory of Surface and Interface Science and Engineering for Catalysts, Zhejiang University of Technology, Hangzhou, 310032, China.
E-mail: lyujh@zjut.edu.cn, dingcr@zjut.edu.cn, xnli@zjut.edu.cn
† These authors contributed equally to this work.

suitable for low-cost and small-scale production of H_2O_2. Prior to this, we also conducted related research on the direct synthesis of H_2O_2 from hydrogen and oxygen.[8,9] The reaction mechanism is that H·, which is formed by the dissociative adsorption of H_2, reacts with OO· formed by non-dissociative adsorption of O_2 to form H_2O_2 through an ·OOH intermediate. There are many hydroperoxides and reactive oxygen species in the reaction process, and the active species of H_2O_2 act on the oxidation reaction. The following section introduces various strategies for *in situ* H_2O_2 generation and, using representative oxidation reactions that are extensively studied both domestically and internationally as examples, reviews the recent progress and key challenges in this field, aiming to provide insights and references for future research.

Jinghui Lyu

Jinghui Lyu is an Associate Professor and PhD supervisor at Zhejiang University of Technology (ZJUT). He received his BS (2006) and PhD (2014) degrees from ZJUT under the supervision of Prof. Xiaonian Li. He worked as a technology and engineering researcher (2006–2008) and as a postdoctoral fellow (2014–2016), contributing to the industrialization of several lab-scale catalytic technologies. From 2019 to 2020, he was a visiting scholar at Western University, Canada. His research focuses on heterogeneous catalysis, particularly the design and application of porous materials (zeolites, MOFs, and COFs) and supported metal catalysts for green chemical processes, including selective hydrogenation, oxidation reactions, and continuous flow catalysis. He has led multiple national research projects in China and successfully transferred patented catalytic technologies to industrial practice.

Han Wu

Han Wu is currently pursuing his PhD in Chemical Engineering at Zhejiang University of Technology, under the supervision of Prof. Xiaonian Li and Associate Prof. Jinghui Lyu. His research interests lie in industrial catalysis, with a focus on green synthesis, catalytic reaction engineering, and the design of transition metal-based catalysts. He is particularly interested in applying heterogeneous catalytic systems to fine chemical production and continuous-flow processes, aiming to enhance catalytic efficiency, selectivity, and sustainability in industrial applications.

Chengrong Ding

Chengrong Ding, born in January 1966, is a Professor-level Senior Engineer and PhD supervisor at the College of Chemical Engineering, Zhejiang University of Technology. He received his bachelor's degree from Dalian University of Technology in 1988 and a master's degree from Zhejiang University in 1996. His research focuses on the synthesis and industrial application of fine chemicals, including pharmaceuticals and pesticides. He has published over 65 papers (50 SCI-indexed), holds 20 patents, and has led more than 20 enterprise projects. His work on continuous-flow processes was recognized with the Zhejiang Provincial Science and Technology Progress Award (Second Prize). He also serves as an expert for multiple Zhejiang provincial departments.

Xiaonian Li

Xiaonian Li, PhD, Professor, is a doctoral supervisor at Zhejiang University of Technology, a Fellow of the Canadian Academy of Engineering, and former President of the university. He received his PhD from the Chinese Academy of Sciences in 1998 and conducted postdoctoral research at the University of British Columbia and Oak Ridge National Laboratory. His research focuses on industrial catalysis and green chemical processes. He has received the National Technological Invention Second Prize and holds several academic roles, including member of the State Council Academic Evaluation Committee and executive director of the Chemical Industry and Engineering Society of China.

2 Approaches to *in situ* H_2O_2 production

Driven by the need for greener and more sustainable chemical processes, the development of efficient methods for H_2O_2 synthesis has become a research focus. Conventional anthraquinone-based processes suffer from complex procedures, high energy consumption, and undesired by-products, limiting their environmental viability. Akram *et al.* pioneered the direct synthesis of H_2O_2 *via* the reaction of H_2 and O_2 over supported bimetallic gold–palladium catalysts. This innovative approach not only simplifies the production pathway but also demonstrates significant advantages in catalytic activity, selectivity, and stability, marking the inception of *in situ* synthesis methods for H_2O_2 production.

2.1 Enzymatic catalysis method

Enzymatic catalysis represents a green and highly selective strategy for *in situ* H_2O_2 generation. Typical systems employ redox enzymes such as glucose oxidase or peroxidases to catalyze the two-electron reduction of O_2 to H_2O_2, offering high substrate specificity and excellent biocompatibility.[10] Operating under mild conditions—ambient temperature and near-neutral pH—this method is particularly suitable for biologically or environmentally sensitive oxidation processes. The generation efficiency and selectivity of H_2O_2 can be further enhanced by optimizing enzyme immobilization strategies, tuning electrode interfaces, and controlling electron transfer mechanisms, including both mediated and direct pathways.[11] Despite its potential, this approach is currently limited by enzyme instability, deactivation tendencies, and relatively low productivity.

2.2 Chemical catalysis method

Chemical catalytic synthesis of H_2O_2 *via* the direct reaction of H_2 and O_2 over noble metal catalysts represents one of the most promising strategies for *in situ* H_2O_2 generation. The mechanism involves dissociative adsorption of H_2 and non-dissociative adsorption of O_2 on the catalyst surface, leading to ·OOH intermediates that subsequently form H_2O_2. Suppressing the undesired hydrogenation of H_2O_2 to water is key to improving selectivity.[12] Studies have shown that the catalyst's metal composition, oxidation state, support material, and reaction environment all significantly influence the activity and selectivity. Alloying,[13] the use of high-surface-area supports such as activated carbon, and fine control over gas–liquid–liquid interfaces in microreactor systems[14] have proven effective in enhancing both the efficiency and the process safety. Moreover, introducing metal or non-metallic additives can modulate the electronic properties of Pd, thereby suppressing the H_2O_2 degradation pathways.[15] This approach offers high atom economy, a short reaction route, and strong compatibility with oxidation processes. However, challenges remain, including catalyst deactivation and the inherent safety risks associated with H_2/O_2 mixtures.

2.3 Ultrasonic method

Ultrasound-assisted contact electro-catalysis has recently emerged as a novel and green strategy for *in situ* H_2O_2 generation, offering advantages such as metal-free operation, environmental compatibility, and structural simplicity. Wang *et al.*[16] reported a catalyst-free system in which the combination of a poly(tetrafluoroethylene) stirring bar and ultrasound induces localized charge separation at the gas–liquid interface, facilitating the two-electron reduction of O_2 to H_2O_2 under ultrasonic excitation, charge accumulation on the PTFE surface mimics the role of an electrode, enabling the formation of reactive oxygen species that subsequently convert into H_2O_2. This approach eliminates the need for noble metals or enzymatic components and operates under mild, low-cost conditions, making it attractive for sustainable oxidation applications. However, current limitations include relatively low H_2O_2 production rates, inefficient interfacial charge separation, and limited system stability.

2.4 Plasma method

Plasma-assisted catalysis offers a non-thermal, high-energy alternative for *in situ* H_2O_2 synthesis by activating molecular species through electron excitation. Zhou *et al.*[17] first demonstrated the direct synthesis of H_2O_2 from H_2 and O_2 using non-equilibrium plasma discharge, in which reactive oxygen species, particularly ·OOH intermediates, are generated in the gas phase under plasma excitation. Subsequent work extended this concept to CH_4/O_2 systems, where methane serves both as a stabilizer for plasma discharge and as a modulator of the H/O ratio, contributing to improved H_2O_2 selectivity.[18] This plasma-based approach operates without traditional catalysts, offering advantages such as rapid start-up, broad operational flexibility, and compatibility with complex gas-phase mixtures. However, challenges remain, including relatively low H_2O_2 yields, high energy consumption, and poor product stability due to harsh oxidative environments.

2.5 Photocatalytic method

Photocatalytic synthesis of H_2O_2 involves the use of semiconductor materials to harness visible light for generating electron–hole pairs that drive the two-electron reduction of O_2. Shiraishi *et al.*[19] reported that graphitic carbon nitride (g-C_3N_4) efficiently catalyzes this reaction under visible light, with high selectivity attributed to its electronic structure, which favors two-electron over four-electron O_2 reduction, thereby suppressing water formation. Building on this, Kofuji *et al.*[20] designed g-C_3N_4-based nanohybrids incorporating aromatic diimides and graphene, forming metal-free heterojunctions that promote charge separation and enable more stable photocatalytic H_2O_2 production, achieving a solar-to-peroxide energy conversion efficiency of 0.2%. This strategy benefits from mild reaction conditions, solar energy utilization, and the absence of applied bias or precious metals, making it particularly

suitable for decentralized and green chemical systems. Nevertheless, limitations remain, including narrow visible light absorption ranges, high recombination rates of charge carriers, and challenges in stabilizing accumulated H_2O_2.

2.6 Electrochemical method

Electrocatalytic synthesis of H_2O_2 *via* the two-electron oxygen reduction reaction represents a promising and sustainable route for *in situ* H_2O_2 generation. This approach relies on applying a controlled potential to drive the selective reduction of O_2 to ·OOH intermediates, avoiding the competing four-electron pathway to water, and thereby, enhancing the H_2O_2 selectivity.[21,22] While early efforts focused on mechanistic understanding and precious metal catalysts,[23] recent advances emphasized the development of non-precious metal systems, particularly nitrogen-doped carbon-based materials and single-site M–N–C structures.[24–26] For instance, atomic-level tuning of coordination environments in Co–N–C catalysts had been shown to modulate the O_2 adsorption geometry and balance the activity–selectivity trade-offs.[25] Electrocatalytic approaches offer several advantages including mild reaction conditions, high energy efficiency, and modular scalability for decentralized applications. However, challenges including catalyst degradation, limited Faradaic efficiency, and instability of H_2O_2 in aqueous media remain.

2.7 Mechanochemical method

Mechanocatalysis has emerged as a novel strategy for *in situ* H_2O_2 generation, driven by mechanical force-induced charge separation without the need for external light, heat, or electrical input. Jin *et al.*[27] demonstrated that ferroelectric $KSr_2Nb_3Ta_2O_{15}$ nanorods can produce surface potential under mechanical agitation, enabling the two-electron reduction of O_2 to H_2O_2 under ambient, dark conditions without any co-catalysts or redox mediators. This method features an energy-free, additive-free system with minimal infrastructure requirements, offering potential for decentralized green oxidation applications. However, current limitations include low H_2O_2 productivity, challenges in controlling the reaction kinetics, and the need to improve the mechanical durability of the catalytic materials. Further mechanistic investigations are required to establish the structure–activity relationships and scalability of this approach.

3 Propylene epoxidation to propylene oxide

3.1 Background

Propylene oxide (PO), a crucial intermediate in chemicals, is widely used to produce polyether polyols, propene glycols, and polyurethane, which are subsequently applied to manufacture polyurethane foams and polyesters. The current annual PO production is more than 10 million tons worldwide, and the demand is increasing remarkably (Scheme 1).[28,29]

The current PO production processes include the chlorohydrin process and the hydroperoxide process (HPPO). Besides, Dong and coworkers[30] explored the epoxidation of olefins by an electro-organic system. Wang *et al.*[31] and Ko *et al.*[32] studied the epoxidation of propylene in a photocatalytic system and a photo-electro-heterogeneous catalytic system. Direct hydrogen peroxide synthesis offers distinct advantages over electrochemical and photocatalytic methods. It typically follows a simple, efficient reaction pathway under ambient temperature and pressure, eliminating the need for high voltages in electrochemical processes or light sources in photocatalysis. This improves energy efficiency and simplifies operations. The catalysts used in direct synthesis show high selectivity, minimizing side reactions, and demonstrate excellent stability, maintaining activity over multiple cycles. Additionally, the process does not require external power or specialized lighting, reducing system complexity and operational costs. However, the chlorohydrin process in the industry produces harmful by-products such as waste salt. As people pay more attention to the environment, the chlorohydrin process which produces harmful by-products is gradually eliminated. Although the hydroperoxide process avoids environmental

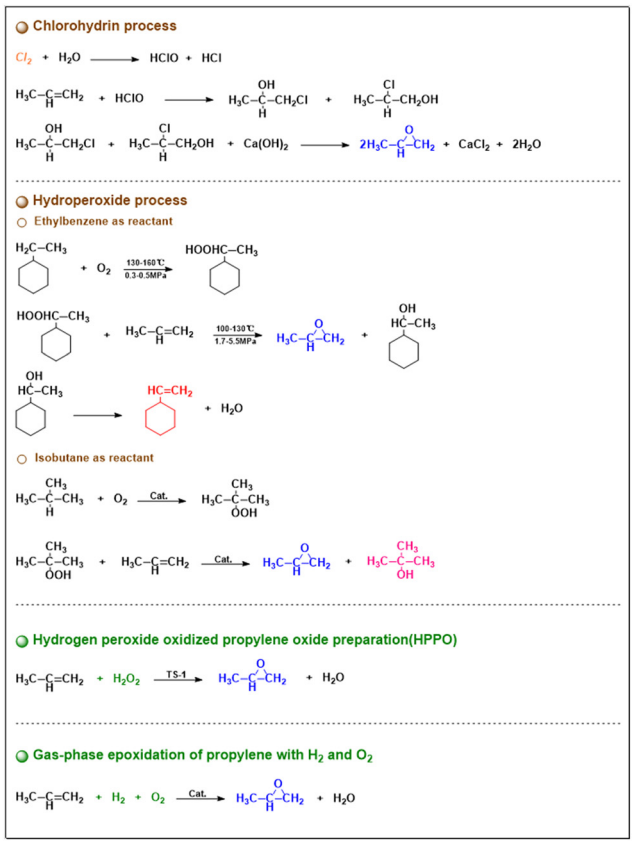

Scheme 1 Various production routes of propylene oxide (PO). Reproduced from ref. 33 with permission from Elsevier, copyright 2021.

pollution, it is not cost-effective due to the lengthy process, high raw material requirements, and many by-products. It is urgent to find alternative production solutions.

H_2O_2, the oxidant used in the direct epoxidation of propylene (C_3H_6) to produce PO (HPPO), is more environmentally friendly, and the only by-product is water. Recently, researchers have obtained a deep understanding of the mechanism of this reaction and have scaled it up to industrial production. However, due to the high cost and risk of transporting H_2O_2, an H_2O_2 manufacturing plant is usually built close to the PO plant to obtain the highest economic benefit. At present, considerable research efforts are dedicated to synthesizing H_2O_2 by H_2 and O_2 first and then consuming it *in situ* to oxidize propylene to PO. Compared with the HPPO process, this gas–solid reaction shows obvious advantages of easy operation, simple product separation, and high economic benefits.[33]

Due to the unique synergy between the Au site and the Ti site, the current research mainly focuses on applying titanium-containing materials loaded with gold nanoparticles as catalysts for the epoxidation of propylene with hydrogen and oxygen. In addition, some researchers try to use Ni (ref. 34 and 35) as an active metal or ZrO_2 (ref. 36) as a support to provide some new strategies. Here, we mainly review the influence mechanism of the structure of gold supported over Ti-based materials as the catalyst on reaction performance and the strategies to improve the catalytic performance in *in situ* propylene epoxidation systems in recent years, such as the influence of metal particle sizes, deposition methods, support structure, and support surface groups on reaction performance.

3.2 Effect of metal

3.2.1 Gold particle sizes. Gold nanoparticles of different sizes have been used in various reactions. Single-atom, gold bilayer, sub nanoclusters, clusters (1–2 nm), and NPs (2–5 nm) were loaded onto different supports and found to have unique characteristics.[37] In the epoxidation of propylene with hydrogen and oxygen, the size effect of Au particles is one of the research focuses. Accurately revealing the effect of gold particle size on the reaction will be helpful to the design of gold catalyst.[38]

Some researchers believe that the size of gold particles should be less than 2.0 nm in the reaction system of *in situ* epoxidation of propylene with hydrogen and oxygen. Qin Zhong and coworkers[39] considered that Au nanoclusters (<1.0 nm) are the primary active sites of gold for propylene epoxidation. Three different supports (titanium silicalite-1 (TS-1), silicalite-1 (S-1)/TS-1, and uncalcined titanium silicalite-1 (unTS-1)) were prepared using the hydrothermal method, and gold was loaded using the DP method. It has been found that the gold nanoclusters (<1.0 nm) on the external surfaces of TS-1 and inside the nanoporous channels of TS-1 are the dominant gold active sites, which is due to its unique catalytic properties. First, gold exhibits high surface energy and abundant active sites at the nanoscale, which effectively activate oxygen molecules to form superoxide species (O_2^-), thereby promoting the selective oxidation pathway of the reaction. Second, gold possesses a weak adsorption ability for C–H bonds, which helps to prevent the side reactions (*e.g.*, deep oxidation) and enhances the selectivity for propylene oxide. Additionally, the surface electronic properties of gold can synergize with supports (such as TiO_2 or SiO_2), further improving the catalytic activity and stability. These characteristics enable gold to achieve both high activity and high selectivity in the epoxidation of propylene, making it the optimal catalyst. In addition, they hope to prepare smaller gold nanoparticles to obtain better catalytic performance. Cheng and coworkers[40] prepared a series of Au/Si/Ti-MCM-36 and Au/Ti-YNU-1 with varying gold loading. They found that the Au nanocluster size of the most efficient catalyst in this series is 1.04 nm. The highly isolated TdTi in Ti-YNU-1 favors the formation of smaller gold nanoclusters.

However, other researchers believe that the optimized size of gold particles should be 2.0–5.0 nm. Feng and coworker[41] found that as the size of the Au particles increased from 2.6 nm to 5.1 nm, the PO selectivity decreased monotonically from 90% to 61%. At the same time, the by-products (such as carbon dioxide, propionaldehyde, ethanol, and acetone) are increasing. Recent advances in nanostructured catalysts demonstrate that confining Au clusters within two-dimensional MXene layers ($Ti_3C_2T_x$) significantly enhances stability and selectivity. For instance, Li and workers designed Au/MXene-TS-1 composites where the MXene's interlayer spacing (≈1.2 nm) restricts Au growth to 2–3 nm clusters. This confinement not only prevents sintering but also facilitates electron transfer from Ti sites to Au, achieving 97% PO selectivity at 200 °C with a record turnover frequency (TOF) of 1200 h^{-1}.[42] *In situ* TEM studies further revealed that MXene's oxygen-terminated surface stabilizes $Au^{\delta-}$ species, which are critical for H_2O_2 activation. To study the size effect of supported Au more effectively, Huang and coworkers[43] loaded Au NPs/clusters on nonporous and highly crystalline TiO_{2-} surface.[44] *Via* a comprehensive *in situ* DRIFTS study, they found that Au particles with sizes of 1.4 to 4.6 nm are mainly composed of the $Au^{\delta-}$ species. An increase in the Au particle size to 5.0 nm increases the active $Au^{\delta-}$–Ti^{4+} ensembles, further increasing the Au particle size to 7.0 nm results in a substantial increase in the $Au^{\delta+}$ species. Li and coworkers[45] synthesized TS-1 *via* a seed-induced method, and bio-inspired Au nanoparticles were loaded through an ionic-liquid-enhanced-immobilization method onto the TS-1 support. They demonstrated that the dosage of the seed introduced during the synthesis of TS-1 significantly affects the acidity of the resulting TS-1, which plays an essential role in regulating the size of the Au NPs (3.0–4.1 nm), and the size of Au nanoparticles within the range of 3.2–3.9 nm was found to be optimal for propylene epoxidation.

The most suitable gold particle size is still controversial, which may be related to supports and deposition methods.

The above-mentioned research explored the effect of gold nanoparticle size on catalytic performance and provided methods and strategies to adjust the size of gold particles in different systems.

3.2.2 Gold deposition method. The loading method of gold can directly impact the loading amount, loading position, and morphology of gold particles. The loading methods of gold include deposition precision (DP), impregnation and ion exchange. DP is the primary method used for loading gold on titanium bearing supports. Ma and coworker[46] found that in the deposition–precipitation process, the surface charge state of the support was changed and the gold loading was increased by adding Ni(II) promoter to Au/TS-1. The gold capture efficiency, catalytic activity, and the relationship between structure and properties were systematically studied. Research by Chen *et al.*[47] indicated that atomically dispersed Au clusters of less than 1 nm can be prepared on TS-1 under the action of NH_3. Li and coworkers[48] prepared a series of Au catalysts supported by amorphous titanosilicate with a three-dimensional wormhole-like mesoporosity (Au/Meso-Ti–O–Si catalysts) by the DP urea method. The DP urea method is a novel and effective way to load Au to assure the dispersion and utilization efficiency of Au NPs on the supports.

Feng and coworkers[49] designed a new route for synthesizing effective gold catalysts by a low-temperature deposition–precipitation method and then studied the formation of gold nanoparticles on the TS-1 support through theoretical and experimental approaches, involving hydrolysis, diffusion, adsorption, and aggregation. It was found that the temperature can influence the spatial position and particle size of gold, and the concept of "effectively accommodated Au clusters" within TS-1. Xiang Feng and coworkers[50] found that the catalytic performance of the Au/TS-1 catalyst is susceptible to the preparation parameters of the deposition–precipitation method. The effect of the charging sequence in the DP process on the catalyst structure and catalytic performance of the Au/TS-1 catalyst was first investigated. For different charging sequences, the compositions of Au complexes and pore properties of TS-1 could affect the transfer of Au complexes into the micropores, resulting in different Au locations and thus significantly different catalytic performance. The results provide direct evidence showing that micropore blocking is the deactivation mechanism.

When gold-based catalysts were prepared by a deposition precipitation method, the alkali source as the gold precipitant was also an essential factor. NH_4OH, NaOH, KOH, CsOH, Na_2CO_3, or Cs_2CO_3 can be used as gold precipitants, especially Na_2CO_3 and Cs_2CO_3. Sodium ions and cesium ions can alter the acidity and alkalinity of the surface of the titanium supports and improve the loading and dispersion of gold. The existence of carbonate anion is also more conducive to the synthesis of PO than the hydroxide anions.

3.2.3 Effect of promoters. A promoter is defined as a substance that does not directly participate in the catalytic reaction but can significantly enhance the activity, selectivity, or stability of a catalyst. Promoters typically exert their influence by modifying the physicochemical properties of the catalyst surface, enhancing the adsorption and activation of reactants, or altering the reaction pathway to yield the desired products. Based on their functions, promoters can generally be classified into three categories: electronic promoters, structural promoters, and surface promoters. Electronic promoters enhance the catalytic activity by modulating the electronic structure of the active sites, thereby influencing charge distribution and reaction kinetics. Structural promoters improve the catalytic performance by modifying the geometric structure of the catalyst, often enhancing stability and dispersion of the active phase. Surface promoters primarily interact with the catalyst surface to increase the adsorption capacity for reactants or to facilitate the conversion of reaction intermediates, thereby improving the overall catalytic efficiency. In the reaction, many metals can play a synergistic role with gold. Ni (ref. 46) helps to improve the loading of gold, Fe (ref. 51) helps to disperse gold, Ag (ref. 52) or Pd (ref. 53 and 54) helps to transfer charge, and Pt (ref. 53) contributes to the desorption of PO to improve the selectivity of PO. A paradigm shift in promoter design was demonstrated by Qiu *et al.*,[55] who developed a ternary Au–Pd–CeO_2/TiO_2 catalyst. The incorporation of CeO_2 as a structural promoter induces the formation of oxygen vacancies, which significantly enhances O_2 dissociation. Meanwhile, Pd selectively donates electrons to Au *via* a strong metal–support interaction (SMSI), further optimizing the catalytic performance. This synergistic effect enables the simultaneous synthesis of H_2O_2 (0.45 mol g^{-1} h^{-1}) and propylene oxide (PO) *via* epoxidation, achieving a PO formation rate of 6200 mmol g^{-1} h^{-1} at 150 °C—representing a 30% improvement compared to the conventional Au/TiO_2 catalysts. Moreover, long-term stability tests over 500 hours

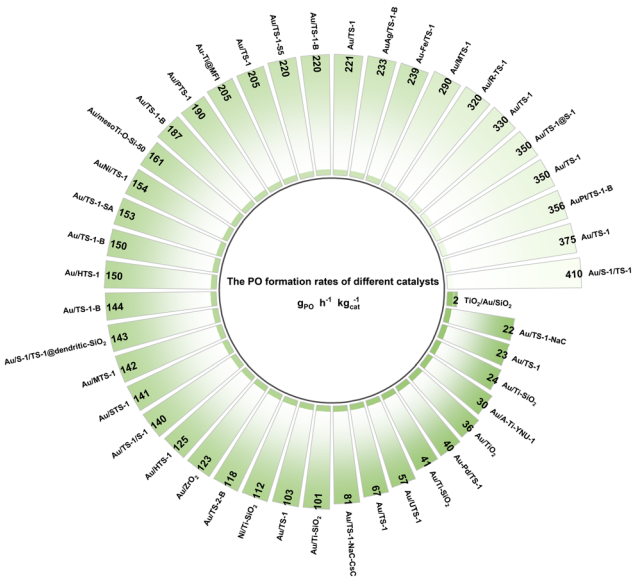

Scheme 2 PO formation rates of different catalysts.

revealed negligible deactivation, which is attributed to the ability of CeO_2 to scavenge reactive oxygen species (ROS), thereby mitigating catalyst degradation. Notably, each promoter exhibits distinct functionalities and plays a unique role in enhancing the overall catalytic efficiency and durability of the system.

3.3 Effect of support

Many titanium-containing materials such as TiO_2, TiO_2–SiO_2, Ti–SiO_2, TS-1, and TS-2 have been used in propylene epoxidation with hydrogen and oxygen. In recent years, the research on TS-1 has increased significantly due to its isolated Ti sites, stable structure, rich pores, and other excellent properties. Research on TS-1 mainly focuses on adjusting its structure and surface groups. The PO formation rates of different catalysts are shown in Scheme 2.

3.3.1 Pore structure of supports. In recent years, many researchers have paid attention to the effect of support pore structure on catalytic performance, and many titanium silicon molecular sieves such as mesoporous titanium silicate-1 (MTS-1),[56,57] small-sized mesoporous titanium silicate-1 (STS-1)[58] and hierarchical titanium silicate-1 (HTS-1)[59,60] have been used to improve the performance of catalysts. The stability and mass transferability of these carriers have been widely recognized. The better mass transferability by shortened reactant/product diffusion length results in lower coke formation and the absence of refractory aromatic coke, inhibiting the side reactions and deactivation caused by the blocking of micropores and active sites. For example, Zhuang *et al.*[61,62] introduced Fe single-atoms into hierarchical TS-1 (Fe-SA/TS-1) by a vapor-phase exchange method. The Fe–N_4 sites adjacent to Ti–O^- centers act as co-catalysts, lowering the activation energy for H_2O_2 formation from 85 kJ mol^{-1} to 62 kJ mol^{-1}. Coupled with the hierarchical pores (micropores: 0.55 nm; mesopores: 5–10 nm), this design achieved 90% H_2O_2 utilization efficiency—40% higher than pure TS-1—by ensuring rapid diffusion of H_2O_2 to Au active sites while minimizing decomposition.

3.3.2 Supports with core–shell structures. The influence of the core–shell structure of the support on the catalytic performance has also attracted much attention in recent years. Many novel catalysts have been designed and applied in the catalyst system of *in situ* epoxidation of propylene with hydrogen and oxygen, such as Au/S-1/TS-1,[39,63] Au/TS-1/S-1,[64] Au/TS-1@S-1,[65] Au–Ti@MFI,[66] and Au/S-1/TS-1@dendritic-SiO_2.[67] These catalysts with core–shell structures have dispersed active sites, excellent mass transferability, and high stability, and some unique sites often appear at the core–shell junction.

3.3.3 Effect of support surface groups. The groups on the surface of the support will also affect the performance of the catalyst. Angelo and coworkers[68] found that hexamethyldisilazane (HMDS) and transition metal dichalcogenides (TMDs) for gas-phase silylation can significantly improve the catalytic performance. Hexamethylenediamine (HMD) improved the yield and selectivity of PO, while TMD treatment completely inhibited the formation of propane. These findings show that the silylation of the catalyst can provide hydrophobicity for the catalyst and promote the desorption of the product but also effectively block the sites of side reactions.

The schematic diagram of catalyst design in propylene epoxidation and experimental parameters and results of different researches are shown in Table 1 and Scheme 3. In the direct gas-phase epoxidation of propylene, Au nanoparticles and titanium-containing supports form a series of bifunctional catalysts. TS-1 has excellent catalytic performance among many titanium-containing supports because of its isolated tetra-coordinated Ti and strong hydrophobicity. In recent years, researchers have carried out comprehensive research and exploration on such catalysts to improve further the catalytic performance and stability of catalysts from the perspectives of gold particle-size regulation and loading, the addition of promoters, pore structure support, core–shell structure, and surface modification. At the same time, they also provide strategies and methods for the follow-up research of this reaction and similar reactions.

3.4 Selective oxidation of ethylene to ethylene glycol *via in situ* H_2O_2

Among diverse olefin oxidation reactions, the selective oxidation of ethylene to ethylene glycol (EG) represents a transformation of considerable industrial significance. As the simplest olefin and a cornerstone petrochemical feedstock, ethylene derivatives are foundational to numerous industrial sectors, making EG production a key indicator of chemical manufacturing capacity.[87,88] Ethylene glycol, the simplest aliphatic diol, is widely used in the synthesis of polyester fibers, plastics, and related materials, and serves as a critical benchmark for assessing industrial chemical development.[89,90]

The choice of oxidant fundamentally governs the efficiency of ethylene-to-EG processes. While molecular oxygen (O_2) is commonly used, its high reactivity often results in the overoxidation to CO_2 and water, complicating downstream separation.[91] Air, though more economical, suffers from lower oxygen content (~21%) and correspondingly reduced selectivity. Process data typically show an EG selectivity of 65–75% when using air, compared to 75–90% with pure O_2, with ethylene conversion rates generally around 8–12%.[92] In contrast, peroxide-based oxidants, particularly hydrogen peroxide (H_2O_2), offer significant advantages by enabling up to 100% selectivity to EG with minimal side-product formation.[93] Furthermore, H_2O_2 decomposes into only water and oxygen, aligning with the principles of green chemistry.

Guan *et al.*[94] established an integrated electrocatalytic tandem system for ethylene-to-EG conversion, employing

Table 1 Summary of various catalytic systems for coupling the epoxidation of propylene with *in situ* generation of H_2O_2

	Catalyst			Experimental conditions				Activity results				
											Reaction rate	
Ref.	Catalyst name	Au loading (wt%)	Au particle size (nm)	Catalyst mass (g)	T (K)	GHSV (ml g_{cat}^{-1} h^{-1})	C_3H_6 : H_2 : O_2 : inert	Propylene conversion (mol%)	PO selectivity (mol%)	H_2 efficiency (mol%)	($mmol_{PO}$ h^{-1} g_{Au}^{-1})	(g_{PO} h^{-1} kg_{cat}^{-1})
43	Au/TiO_2	5	5 ± 1.6	0.25	323.15	8000	1 : 1 : 1 : 7	1.8	96.8	33	12.52	36.3
69	$Au/Ti–SiO_2$	0.18	2.3 ± 1.0	0.15	473.15	10 000	1 : 1 : 1 : 7	2.2	89.3	4.8	396.55	41.4
68	$Au/Ti–SiO_2$	0.15	—	0.15	493.15	10 000	1 : 1 : 1 : 7	4.7	83	11	1160.92	101
70	$Au/Ti–SiO_2$	0.03	2.4 ± 0.6	0.15	473.15	14 000	1 : 1 : 1 : 7	0.8	84.9	12.8	1390.80	24.2
71	Au/TS-1	0.24	—	0.15	473.15	14 000	1 : 1 : 1 : 7	12	87	25	2693.97	375
72	Au/TS-1	0.314	5.1 ± 4.7	0.15	473.15	14 000	1 : 1 : 3 : 5	—	98	26	1921.81	350
39	Au/TS-1	0.1	—	0.15	473.15	14 000	1 : 1 : 1 : 7	10.5	87	10	5689.66	330
73	Au/TS-1	2	3.7	0.1	473.15	9000	1 : 1 : 1 : 7	5.2	84.83	25	88.74	102.94
74	Au/TS-1	0.15	2.1 ± 0.3	0.15	473.15	8000	1 : 1 : 1 : 17	8.4	81.3	14.2	765.52	66.6
45	Au/TS-1	—	3.2 ± 0.5	0.15	578.15	7000	1 : 1 : 1 : 7	19	70.5	72	—	221
29	Au/TS-1	1	3.0 ± 0.8	0.5	473.15	8000	1 : 1 : 1 : 7	1.3	88	23	38.79	22.5
49	Au/TS-1	0.1	2.4 ± 0.5	0.15	473.15	14 000	1 : 1 : 1 : 7	—	83	—	3534.48	205
54	Au–Pd/TS-1	0.76	3.9 ± 0.6	0.15	473.15	14 000	1 : 1 : 1 : 7	—	42	—	90.74	40
51	Au–Fe/TS-1	0.69	3.1 ± 0.2	0.15	473.15	14 000	1 : 1 : 1 : 7	7.3	89.9	25.7	596.70	238.8
46	AuNi/TS-1	0.212	3.5 ± 0.6	0.15	443.15	14 000	1 : 1 : 1 : 7	10.3	73	31	1252.44	154
75	Au/TS-1-B	0.09	2.8 ± 0.5	0.15	473.15	14 000	1 : 1 : 1 : 7	—	91	40	2758.62	144
76	Au/TS-1-B	0.5	4.6 ± 0.5	0.15	578.15	7000	1 : 1 : 1 : 7	14.5	73.7	28	644.83	187
77	Au/TS-1-B	—	3.1 ± 0.6	0.15	473.15	14 000	1 : 1 : 1 : 7	—	88	37	—	150
41	Au/TS-1-B	0.13	2.6 ± 0.5	0.15	473.15	14 000	1 : 1 : 1 : 7	9	70	15	2917.77	220
52	AuAg/TS-1-B	0.08	2.8 ± 0.5	0.15	493.15	14 000	1 : 1 : 1 : 7	—	73	44	5021.55	233
78	AuPt/TS-1-B	0.1	3.2 ± 0.7	0.15	473.15	14 000	1 : 1 : 1 : 7	11	88	41	6137.93	356
50	Au/TS-1-SA	0.15	2.8 ± 0.5	0.15	473.15	14 000	1 : 1 : 1 : 7	—	90	15	1758.62	153
79	Au/TS-1-S5	0.5	3.8 ± 0.6	0.15	573.15	7000	1 : 1 : 1 : 7	18.3	72.6	32.2	757.59	219.7
80	Au/TS-1-NaC-CsC	0.21	2.7 ± 0.9	0.15	473.15	8000	1 : 1 : 1 : 17	9.2	91.2	18.1	665.02	81
81	Au/TS-1-NaC	0.25	1.9 ± 0.5	0.1	483.15	14 000	1 : 1 : 1 : 55.5	—	95	—	151.72	22
82	Au/TS-2-B	0.09	2.9 ± 0.4	0.15	473.15	—	1 : 1 : 1 : 7	—	91	35	2260.54	118
59	Au/HTS-1	0.1	3.2 ± 0.2	0.15	473.15	—	1 : 1 : 1 : 7	—	85	—	2155.17	125
60	Au/HTS-1	0.1	3.0 ± 0.3	0.15	473.15	14 000	1 : 1 : 1 : 7	—	90	—	2586.21	150
57	Au/MTS-1	0.13	3.4 ± 0.5	0.15	473.15	14 000	1 : 1 : 1 : 7	—	95.2	—	1883.29	142
56	Au/MTS-1	0.324	—	0.15	473.15	14 000	1 : 1 : 1 : 7	—	95	—	1543.21	290
83	Au/PTS-1	0.17	—	0.15	473.15	14 000	1 : 1 : 1 : 7	6.8	91	—	1926.98	190
58	Au/STS-1	0.1	3.1 ± 0.4	0.15	473.15	—	1 : 1 : 1 : 7	—	91.2	—	2431.03	141
84	Au/UTS-1	0.031	—	0.15	473.15	14 000	1 : 1 : 1 : 7	1.08	97	24	3170.19	57
85	Au/R-TS-1	—	1.98	0.15	473.15	14 000	1 : 1 : 1 : 7	—	86	20	—	320
86	$TiO_2/Au/SiO_2$	0.7	—	0.15	373.15	14 000	1 : 1 : 1 : 7	—	90	—	3.69	1.5
40	Au/A-Ti-YNU-1	0.13	1.5 ± 0.5	0.25	498.15	7000	1 : 1 : 1 : 7	3.3	59.3	36.2	397.88	30
48	Au/mesoTi–O–Si-50	0.5	2.4 ± 0.3	0.15	573.15	7000	1 : 1 : 1 : 7	12.8	76.2	18.2	554.83	160.9
64	Au/TS-1/S-1	0.1	2.9 ± 0.3	0.15	473.15	14 000	1 : 1 : 1 : 7	—	87.2	—	2413.79	140
63	Au/S-1/TS-1	0.326	—	0.15	473.15	14 000	1 : 1 : 1 : 7	6.7	96	15	2168.39	410
65	Au/TS-1@S-1	0.326	4	0.15	473.15	—	1 : 1 : 1 : 7	—	—	—	105.00	350
67	Au/S-1/TS-1@dendritic-SiO_2	0.1	2.9 ± 0.3	0.15	473.15	14 000	1 : 1 : 1 : 7	4.18	93.9	26.1	2472.41	143.4
66	Au–Ti@MFI	0.5	—	0.15	573.15	7000	1 : 1 : 1 : 7	14.8	83.9	—	706.90	205
34	$Ni/Ti–SiO_2$	1	3.2 ± 0.4	—	473.15	10 000	1 : 1 : 1 : 7	7.5	90.7	16.3	—	112
36	Au/ZrO_2	0.017	3.6 ± 0.6	0.15	423.15	8000	1 : 1 : 1 : 7	0.14	42.3	—	124.40	122.65

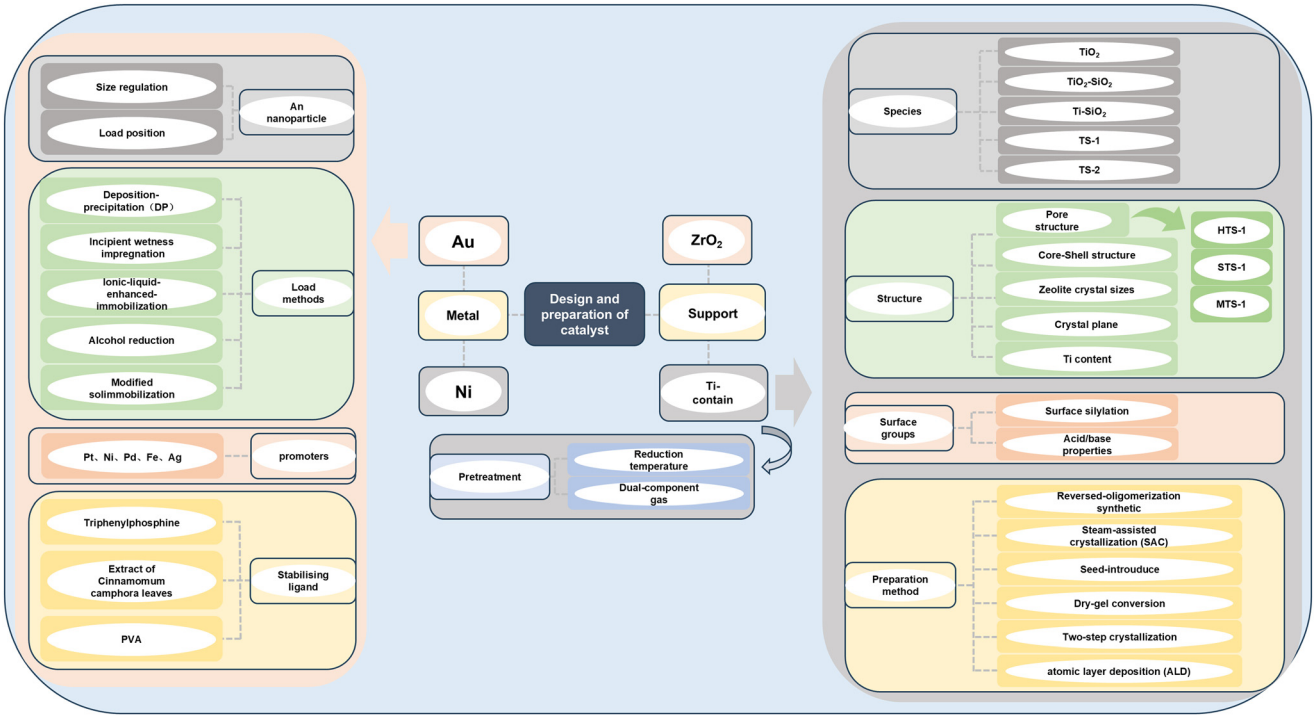

Scheme 3 Design framework of the propylene epoxidation catalyst.

electrocatalytic oxygen reduction on mesoporous carbon (MC-3) to generate H_2O_2 *in situ*, followed by immediate ethylene oxidation over TS-1 zeolite. Their approach achieved 99% EG selectivity and 86% H_2O_2 conversion under ambient temperature and pressure, effectively circumventing the high energy demands of conventional processes and eliminating the risks associated with H_2O_2 storage and transport. The use of noble-metal-free catalysts further highlights the sustainability and scalability of this method.

In addition, Yang *et al.*[95] engineered a vanadyl phthalocyanine-functionalized catalyst (VOPc/CNT-OH) for highly selective H_2O_2 production in acidic media. Industrial feasibility was demonstrated through continuous operation exceeding 100 hours in flow cell and solid-state electrolyte (SSE) reactors. The electrogenerated H_2O_2 was successfully utilized for ethylene oxidation to EG, validating the practicality of coupled electrocatalytic–thermocatalytic systems.

Consequently, *in situ* reaction coupling strategies offer compelling advantages, including process simplification, the elimination of H_2O_2 storage and transportation hazards, and improved economic viability. These developments demonstrate significant potential for industrial implementation in sustainable EG production.

4 Hydroxylation of benzene to phenol

Phenol is an essential intermediate product widely used in synthesizing resins, drugs, dyes, and other fields. The global phenol market has been valued at over $20 billion in recent years and is expected to maintain a considerable growth rate before 2025.[96] Over 90% of the phenol synthesized today is made by the three-step cumene process, which includes a high-energy condition. Initially, the cumene produced through the alkylation of benzene with propylene is oxidized to cumene hydroperoxide. Then, the phenol and by-product acetone are produced through the hydrolysis of cumene hydroperoxide. The cumene process has a low phenol yield and suffers from low atomic utilization, environmental unfriendliness, high energy consumption, multiple steps, and large amounts of by-products. This method faces high by-product separation costs when separating the by-product acetone.

Furthermore, the risk of explosion potentially exists in the cumene process. To address these challenges, an alternative method called direct hydroxylation of benzene to phenol (DHBP) has been proposed. This direct hydroxylation of benzene remains one of the most challenging catalytic reactions since the benzene ring must be broken in this process.[97]

4.1 Direct hydroxylation of benzene to phenol

O_2, N_2O, and H_2O_2 are the common oxidants utilized in the DHBP process due to their exceptional oxidation capabilities. As early as 1983, Iwamoto *et al.*[98] reported the application of N_2O on V_2O_5–SiO_2 catalysts, achieving 11% conversion of benzene and 45% yield of phenol. Although the unique oxidation effects are obtained by adopting N_2O (ref. 99 and 100) and H_2O_2,[101–103] their practical applications are limited

due to their operating condition and material costs. However, DHBP is available by using O_2 as an oxidant instead. The direct synthesis of phenol from benzene and oxygen requires the activation of the C–H bond in the aromatic ring and the subsequent insertion of oxygen. The oxidation of benzene *via* an electrophilic reaction requires the oxygen species with a negative charge provided in most heterogeneous catalysts containing transition metals such as O^-, O^{2-}, and O^{2-}.[104]

Because of the considerable economic and environmental advantages of this method, direct oxidation of benzene to phenol by using a mixture of H_2 and O_2 has been widely studied. However, many reports show high phenol selectivity using gaseous H_2 and O_2 as reactants but still low phenol yields, or very low phenol selectivity but relatively high yields. Besides, due to a mixture of H_2 and O_2, the risk of explosion should be considered seriously.

4.2 Pd membrane reactor

In this system, H_2 and O_2 are supplied separately on each side of the membrane to avoid contact in the gas phase. In addition, only H_2 can pass through the dense Pd membrane, while O_2 cannot. *In situ* H_2O_2 and other reactive oxygen species (such as HOO· and HO·), which are able to promote the conversion of benzene to phenol, are generated while oxygen is reacting with the dissociated hydrogen that permeates out of the one side of the Pd membrane.[105–108] Thus, this kind of Pd membrane reactor is considered an economic, clean, and valuable technology.

The palladium membranes can be prepared by chemical vapor deposition (CVD) or electroless plating (ELP). CVD is suitable for industrial applications requiring high-quality, complex structures, and large-area films, while ELP is more suited for small-scale production, where the membrane quality is less critical. Noteworthily, the Pd membrane is not only a catalyst but also a hydrogen separator. In contrast to conventional Pd-loaded catalysts in porous supports, the surface area of the Pd membrane is relatively small. The application of Pd membranes in direct catalytic hydroxylation of benzene to phenol is rapidly gaining plenty of attention after Niwa reported this kind of membrane reactor. However, the phenol yields of many studies are not satisfactory.[109–118] Zhang *et al.*[119] employed operando X-ray absorption spectroscopy (XAS) and surface-enhanced Raman spectroscopy (SERS) to track the dynamic evolution of Pd species during the reaction. They identified a reversible $Pd^0 \leftrightarrow PdO_X$ transformation cycle, where Pd^0 domains (2–3 nm) facilitate H_2 dissociation, while PdO_X interfaces (PdO/PdO_2) stabilize HOO· intermediates. By precisely controlling the H_2/O_2 ratio at 2/1, the Pd^0/PdO_X ratio was optimized to 3/1, yielding 22.3% phenol with 98% selectivity—a 50% improvement over previous membrane reactors. Vulpescu *et al.*[118] pointed out that commercial application of Pd membranes is possible through computer simulations if the productivity of phenol and the low efficiency of raw materials are solved. The formation of many by-products was demonstrated to occur *via* two significant side reactions that dominate under the applied experimental conditions. These two reactions are the complete oxidation of hydrogen to water and the complete oxidation of benzene to carbon dioxide. Besides, Niwa *et al.*[105] found membrane deterioration by releasing the Pd layer from the alumina support tube, and Vulpescu *et al.*[118] and Shu *et al.*[114] reported that hot spots can lead to membrane deterioration under oxygen-enriched conditions. Non-selective oxidation and complete combustion occur in a higher oxygen content. However, a higher hydrogen content favors hydrogenation reactions.[117,118,120] Moreover, Sato *et al.*[104] indicated that two phases of palladium hydride with different cell sizes coexist, that is, α-phase and β-phase at below 566.15 K, leading to embrittlement of the Pd membrane. Currently, outstanding results were reported by Wang *et al.*[97,106,121–123] through a systematic study of the membrane, parameters, and feed mode (Table 2).

Even though the Pd membrane reactor has shown encouraging results, space for further commercialization improvement exists due to weaknesses such as membrane deterioration and hot spots, poor membrane stability, and low feedstock utilization.

5 Selective oxidation of methane into oxygenates

The resources of methane are diverse. The main existing form of methane is natural gas, and it makes up nearly 90% of natural gas.[124] The reserves of natural gas are abundant on the earth. It is plentiful in the crust around the world, constituting approximately 21% of the total principal energy sources on earth.[125] The development of simple processes for upgrading natural gas to value-added chemicals is therefore highly desirable.[126] The functionalization of methane to valuable hydrocarbons and oxygen-containing products is

Table 2 Comparison of different results about DBHP over Pd-based membrane reactors

Ref.	Membrane system	Method	T (K)	Benzene conversion (%)	Phenol selectivity (%)	Phenol yield (%)	Long-term (h)
106	Pd-TS-1 membrane	ELP	473.15	7.3	95	6.9	100
106	Pd capillary membrane	ELP	473.15	19	86	16.3	100
123	Pd capillary membrane	ELP	523.15	22.4	76	17.1	140
122	Pd-TS-1p membranes	ELP	473.15	7.2	99	7.1	na.
97	Pd-TS capillary membrane	ELP	473.15	23.4	95	22.3	110
121	Pd-TSH membrane	ELP	473.15	21.9	98	21.4	120

meaningful. Mainly, selective oxidation of methane to methanol is one such process that has received significant attention.[127]

Methane (CH_4) is the simplest saturated hydrocarbon with a standardized tetrahedral structure. The strong C–H bond (104 kcal mol^{-1}, 1 cal = 4.18 J) with negligible electron affinity causes difficulty in C–H activation under mild conditions. The methanol product is also more active than methane and is more prone to overoxidation. Consequently, selective methane oxidation to methanol under mild conditions has been considered a dream reaction (Scheme 4).[128]

Conventionally, an indirect route for converting natural gas to methanol is used. The process has two steps: (1) intermediate production of synthesis gas by steam reforming and (2) catalytic conversion of synthesis gas to methanol. However, syngas production is an energy-intensive process, operated at 65% thermodynamic efficiency between 1073.15 and 1273.15 K, and more than 25% of the feed (natural gas) has to be burned to provide the heat for reaction. There are drawbacks such as complex process flows, low raw material utilization, high carbon emissions, and short catalyst lifespan. Hence, from the viewpoint of sustainable development, the direct conversion of methane to methanol is a desired alternative to the current technology.[124]

In order to achieve the direct oxidation of methane to methanol, several relatively expensive and toxic oxidants have been employed with catalysts, such as fuming sulfuric acid with Hg or Pt catalysts and selenic acid with Au and Pt catalysts. This method could produce methanol and over-oxides and environmentally harmful by-products. The metal-exchanged zeolite catalysts could catalyze the methane oxidation using N_2O, O_2, or even H_2O, which efficiently inhibited the methanol overoxidation, but still required a reaction temperature of 200 °C or higher.[128] H_2O_2, an environmentally friendly oxidant, has significant advantages in methane oxidation under mild conditions without any toxic salts or strong acids. Using H_2O_2 as an oxidant in the direct methane-to-methanol conversion holds potential for improved efficiency and reduced environmental impact, though challenges remain in catalyst stability, cost, and scaling up for industrial production. However, H_2O_2 is expensive relative to gaseous oxygen. In addition, H_2O_2 in the presence of O_2 has been used in the selective oxidation of methane under mild conditions to lower the production costs.[129]

For further control of the cost of this reaction, recent exploration was performed in combining the selective oxidation of methane with the *in situ* generation of H_2O_2 using H_2 and O_2 (Table 3).

Hutchings and co-workers[130–134] have demonstrated that titania-supported AuPd nanoparticles, prepared by the incipient wetness impregnation method, can effectively catalyze the oxidation of methane in water to produce methyl hydroperoxide, methanol, and CO_2 using externally supplied H_2O_2. Moreover, the reaction can be performed using H_2O_2 generated *in situ* from H_2 and O_2 introduced into the gas-phase reaction mixture. Notably, comparable productivity but significantly improved methanol selectivity was observed when employing H_2O_2 generated *in situ*, relative to the use of preformed H_2O_2. This strategy not only simplifies the overall process by eliminating the need for external H_2O_2 supply but also reduces operational costs and minimizes environmental impacts. The *in situ* generation of H_2O_2 offers a more sustainable and economically viable oxidant alternative, while broadening potential applications in areas such as wastewater treatment, carbon capture and utilization, and the production of fine chemicals.

Tsubaki and co-worker[135,136] have reported an Au–Pd catalyst supported on carbon materials (CNTs, AC, and rGO) to convert methane into methane oxygenates with *in situ* generated H_2O_2. In particular, the CNT (carbon nanotube)-supported Pd–Au nanoparticles exhibit excellent catalytic performance in converting methane to methanol. They deduced that weak interaction resulting from CNT supports is more beneficial to the methanol productivity and selectivity. This strategy might facilitate the catalyst designs for this direct conversion of methane to methanol or other catalytic reactions in the future. They also discovered that the methanol productivity increases as the amount of Au loading in the Pd–Au/CNT catalyst increases. More in-depth investigation of this Pd–Au nanoparticle catalyst may facilitate the catalyst design and preparation for this direct

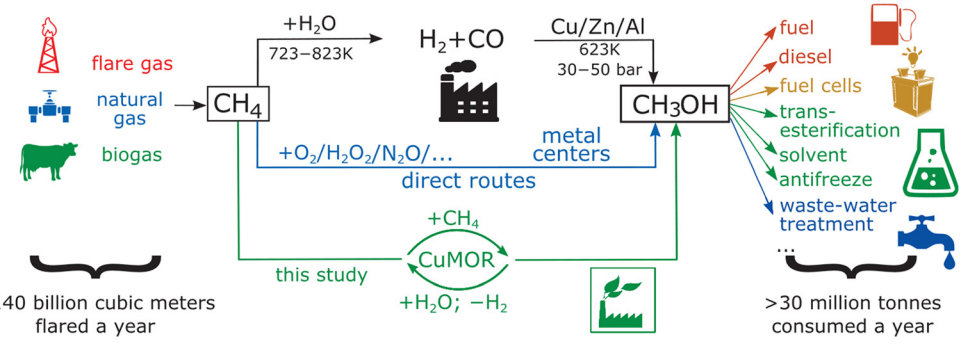

Scheme 4 Current and proposed chemical processes for converting methane to methanol. Reproduced from ref. 127 with permission from the American Association for the Advancement of Science (AAAS), copyright 2017.

Table 3 Summary of various catalytic systems for coupling the oxidation of methane with *in situ* generation of H_2O_2

		Experimental conditions						Activity results			Selectivity			
Ref.	Catalyst	Catalyst mass (mg)	$V_{solution}$ (ml)	T (K)	Time (h)	Gas composition $CH_4/H_2/O_2$/insert	Total pressure (bar)	Total product (mmol g_{metal}^{-1} h^{-1})	CH_3OH amount (μmol)	CH_3OH product (mmol $g_{metal}^{-1}h^{-1}$)	CH_3OH	HCOOH	CH_3OOH	CO_2
132, 134	2.5%Au2.5%Pd/TiO_2	28	10	323.15	0.5	0.86/1.72/75.86/21.55	32	2.32	1.31	1.58	68.2%	0	15.1%	16.7%
135, 136	2.5%Au2.5%Pd/CNTs	30	10	323.15	0.5	47/4/8/41	33	7.60	4.17	5.56	73.2%	22.3%	4.6%	0
142	AuPd@ZSM-5-C_{16}	27	10	343.15	0.5	3.3/6.6/1.6/88.3	30	99.45	64.1	91.6	92.1%	4.3%	Trace	Trace
137	$FeSO_4$ + 1%Pd/C	0.37 mM + 50	30	293.15	0.5	15/3/2.1/7.9	28	—	11	—	3.1%	60.6%	1.9%	34.4%
138	0.9%Fe-ZSM-5 + 1%Pd/AC	50 + 50	30	303.15	0.5	15/3/2.1/7.9	28	400 (Fe)	22	97.6	24.4%	57.8%	0	17.8%
139	0.9%Fe-ZSM-5 + 2%Pd/c-s-HCPP	50 + 25	30	323.15	1	15/3/2.1/7.9	28	185 (Fe)	24	51.8	28%	62%	0	11%

methane to methanol reaction or other catalytic processes in the future.

Park and coworkers[137–139] reported enhanced methane oxygenation when H_2 was introduced in the presence of both $FeSO_4$ and Pd/C. They attributed this to Fe^{2+} accelerating hydroxyl radical (·OH) formation, analogous to a Fenton-like mechanism. These radicals selectively oxidize methane to methane oxygenates. This highlights the superior efficiency of *in situ* H_2O_2 generation over direct H_2O_2 addition.

However, homogeneous Fe catalysts suffer from issues such as metal leaching and recovery challenges. To address this, Fe-ZSM-5 zeolites were explored as heterogeneous alternatives. While lower pH promoted H_2O_2 formation and stability, ICP analysis revealed increased iron leaching under acidic conditions, compromising catalyst durability.[140]

To overcome these limitations, Park *et al.* developed a bifunctional system combining Fe-ZSM-5 with Pd/C supported on an acid-functionalized hyper-crosslinked porous polymer (Pd/c-s-HCPP). The acidic sites on HCPP facilitated *in situ* H_2O_2 generation without external acid. This system achieved high methane conversion and selectivity under mild conditions, while enhancing catalyst stability.

Similarly, Yin *et al.*[141] designed Fe single-atom catalysts on N-doped carbon (Fe-SA/NC) with axial oxygen ligands (Fe–N_4–O). *In situ* FTIR and DFT studies showed that Fe–O bonds polarized the C–H bond in methane, reducing activation energy to 0.8 eV. At 50 °C and 10 bar $CH_4/H_2/O_2$ (3 : 1 : 1), the catalyst delivered 98% methanol selectivity with a space–time yield of 1.2 g L^{-1} h^{-1}, outperforming enzymatic systems. The robust Fe–N coordination suppressed metal leaching, maintaining 95% activity after 100 cycles.

Furthermore, bimetallic Fe–Pd catalysts exhibit synergistic effects, enhancing the degradation of organic pollutants and recalcitrant contaminants. Fe facilitates electron transfer, while Pd accelerates key reaction steps, allowing efficient operation under mild conditions with reduced energy input. These systems not only remove toxic pollutants and heavy metals from wastewater but also enable resource recovery, promoting sustainable chemical processes.

Xiao and coworkers[142] recognized the importance of local H_2O_2 concentration in methane oxidation by *in situ*-generated H_2O_2 under mild conditions. Then, they proposed a molecular fence concept and designed a series of AuPd@zeolite-R catalysts. Au–Pd alloy nanoparticles were embedded in aluminosilicate zeolite crystals that rendered the external surface of the zeolite hydrophobic by appending organosilanes (R). Hydrogen, oxygen, and methane were easy to diffuse to the catalytically active sites to form H_2O_2, but the generated H_2O_2 was difficult for diffusing out of the zeolite crystals. The hydrophobic sheath hinders H_2O_2 diffusion from the encapsulated AuPd nanoparticles, enhancing its concentration in the zeolite crystals, thereby achieving excellent catalytic effects. The concept of a molecular fence opened a productive route to efficient catalysts for partial methane oxidation.

Several groups reported successful partial methane oxidation using H_2O_2 generated *in situ* from hydrogen and oxygen and put forward some exciting concepts. However, the mechanism of partial methane oxidation should be further explored. We can design highly active catalysts that match the reaction with a complete understanding of the methane oxidation pathway.

6 Green adipic acid synthesis

Adipic acid, an important industrial dicarboxylic acid, has attracted considerable attention in recent years for its green synthesis, particularly *via* oxidation routes of cyclohexene or cyclohexane driven by *in situ*-generated H_2O_2. Sato *et al.*[143] pioneered a "green" route employing 30% H_2O_2 for the direct oxidation of cyclohexene to high-purity adipic acid under mild conditions, achieving yields up to 93% while completely eliminating harmful N_2O emissions associated with traditional nitric acid methods. This work laid the foundation for H_2O_2-based adipic acid synthesis.

Ribeiro *et al.*[144] compared the oxidation performances of cyclohexene and cyclohexane, highlighting that the presence of the C=C double bond in cyclohexene facilitates adipic acid formation under H_2O_2 and microwave-assisted conditions, reaching yields of 46%. In contrast, the activation of the C–H bond in cyclohexane is more challenging, resulting in lower efficiency. Their study also demonstrated partial recyclability of a C-chelated iron catalyst in ionic liquids, enhancing the sustainability of the catalytic system.

Van *et al.*[145] reviewed emerging catalytic processes for green adipic acid synthesis, emphasizing that coupling *in situ* H_2O_2 generation with oxidation reactions improves efficiency and reduces risks associated with the storage and transportation of concentrated H_2O_2. Furthermore, Noyori *et al.*[146] summarized design principles and catalyst optimization strategies for aqueous-phase H_2O_2 oxidation systems, advancing the development of tungstate and related catalysts.

From a biocatalytic perspective, Li *et al.*[147] reviewed peroxygenase-driven C–H functionalization reactions, focusing on *in situ* H_2O_2 generation *via* electro- and photocatalytic methods. They highlighted the critical importance of precise control of H_2O_2 concentration to enhance the reaction efficiency and prevent enzyme deactivation.

In summary, current research on green adipic acid synthesis mainly concentrates on designing efficient catalytic systems based on hydrogen peroxide and *in situ* H_2O_2 generation technologies. By integrating traditional and biocatalytic approaches and optimizing reaction systems and catalysts, significant progress has been made toward environmentally friendly and sustainable industrial production of adipic acid.

7 Fenton process

When phenolic compounds are widely used as essential chemical raw materials and intermediates, a large amount of industrial phenol-containing organic wastewater that is difficult to degrade is generated. Untreated organic wastewater discharged directly into water bodies or soil can adversely affect aquatic organisms and soil diversity due to the presence of chemicals such as organic solvents, dyes, and pesticide residues. The Fenton synthesis process offers an economic and environmentally friendly solution for organic wastewater treatment through the efficient degradation and resource utilization of organic pollutants. It can convert organic components in wastewater into clean fuels, reducing environmental pollution, promoting circular economy development, and achieving dual benefits of wastewater treatment and resource utilization.

In recent years, there have been many studies on the Fenton reaction with H_2O_2, mainly Pd-based and Fe-based catalysts,[148–157] all of which can be used for the degradation of insoluble organic compounds and have achieved good results.

Fenton technology has made many advances in the field of water contaminant control. The current oxidant used, H_2O_2, is very costly, but its transportation and storage costs are incredibly high, so there is an urgent need to find a solution for it.

In analogy to reactions such as epoxidation of propylene and hydroxylation of benzene, perhaps the *in situ* participation of hydrogen and oxygen in the Fenton reaction compared to the direct participation of H_2O_2, the raw material of this system is not only easier to store but also allows the *in situ* production of H_2O_2 from electrically generated H_2 and O_2 using catalysts such as Pd/C. These studies demonstrate the great potential of *in situ*-generated H_2O_2 in waste treatment oxidation reactions, reducing the current costs associated with H_2O_2 production. Furthermore, it is essential to highlight that the use of bimetallic Fe–Pd catalytic systems can improve the degradation performance and reduce the environmental impact of the process through the heterogeneity of Fenton ferrous ions and their associated synergistic effects.

8 Oxidative desulphurization

In numerous countries, coal has always been dominant, and the combustion of fossil fuels will bring severe environmental pollution, such as the issue of acid rain caused by SO_2 emissions, which can easily disrupt the soil's acid–base balance, leading to a rapid reduction in crop yields and a severe threat to people's lives. Waste tires contain a large number of sulfur components. Many countries in Europe have banned tire disposal in landfills.[158] High sulfur contents reduce the quality of refined oil and poisonous catalysts, shortening their lifespan and activity. Additionally, sulfur pollution poses health risks, as prolonged exposure to

sulfur dioxide can cause respiratory diseases such as asthma and bronchitis. A notable example is the "Great Smog of London" in the mid-20th century, where extensive coal burning released large amounts of sulfur dioxide, leading to severe air pollution and thousands of deaths from respiratory and cardiovascular diseases. Therefore, reducing sulfur emissions is a critical issue. It is essential to promote energy conservation, implement strict sulfur dioxide emission controls, and develop cost-effective desulfurization technologies. Many researchers are dedicated to advancing desulfurization efforts.

The main application areas of oxidative desulfurization are addressing issues in the combustion of fossil fuel coal and pyrolysis of waste tires. Common desulfurization technologies encompass hydrodesulfurization, oxidative and biological desulfurization, adsorption, and ionic liquid extraction.[159] In the study of pyrolysis of waste tires, the central technology used in the past was hydrodesulfurization, which had disadvantages of high reaction temperature, high hydrogen pressure, large reactor volume, and high catalyst requirements.[160] Absolutely, oxidative desulfurization has emerged as a viable solution for mitigating sulfur-related issues in fuels. It utilizes H_2O_2 as an oxidant, which is cost-effective and readily available. Notably, oxidative desulfurization offers environmental advantages over hydrodesulfurization; first, the technology is centered on selective oxidation, converting sulfides into soluble or separable sulfur derivatives, such as sulfuric acid or elemental sulfur, thereby achieving efficient desulfurization. It typically operates under relatively low-temperature and -pressure conditions, significantly reducing energy consumption. Second, oxidative desulfurization avoids common issues associated with absorption methods, such as the regeneration of absorbents and physical adsorption methods, such as adsorption saturation, resulting in relatively lower operating costs. Additionally, the byproducts of oxidative desulfurization are mostly non-toxic and recyclable substances, such as elemental sulfur, facilitating resource utilization. Compared with the traditional chemical desulfurization methods, it greatly reduces the risk of secondary pollution.[161] Indeed, Fe-based nanoparticles catalysts have shown promise in desulfurization processes.[162] Additionally, the inclusion of H_2O_2 can enhance the desulfurization efficiency,[160] leading to shortened reaction times. H_2O_2 exhibits the ability to effectively eliminate inorganic sulfur during coal combustion, contributing to cleaner and more efficient energy production.[163]

The utilization of supported catalysts has expanded to encompass the catalysis of thiophene compounds alongside H_2O_2. Studies have showcased remarkable desulfurization efficiency.[158] These catalysts exhibit recyclability across multiple reactions while maintaining stable activity. For instance, Li *et al.* used SiO_2-supported $H_3PMo_{12}O_{40}$ and H_2O_2 for catalyzing dibenzothiophene and diesel desulfurization, demonstrating sustained excellent performance even after numerous cycles.[164] Xie *et al.*[165,166] enabled continuous oxidative desulfurization with 98.7% sulfur removal efficiency, leveraging *in situ* H_2O_2 generation and instantaneous mixing at the microscale. Another study by Qi *et al.* focused on HPW/PEHA/Zr SBA-15 catalysis of dibenzothiophene, further contributing to the advancements in desulfurization processes.[167]

Absolutely, desulfurization technologies are rapidly evolving toward cost-effectiveness, reduced pollution, higher efficiency, and environmental friendliness. Presently, oxidative desulfurization technology remains a dominant method due to its effectiveness. However, other approaches such as adsorption, extraction, and biological desulfurization are also advancing, showing promising developments. This diversification in desulfurization techniques signifies a rapid expansion in the desulfurization industry.

9 Oxidation of sulfides to sulphones

Sulfone plays an essential role in modern organic chemistry. They are highly versatile components and can be used in various applications such as drugs, agrochemicals, or functional materials.[168] In recent years, sulfone electrolytes have gained great interest because of their wide electrochemical window and high safety.[169] Many natural organic synthesis products, drugs, and crop protection chemicals contain sulfone or sulfoxide functional groups. Sulfones and sulfoxides are widely used in pharmaceutical, agricultural, biological, chemical, and industrial fields because of their unique biological and chemical activities.

The four traditional and most common methods for the synthesis of sulfones are the oxidation of sulfides (or sulfoxides), the Foucault reaction with a sulfonyl chloride, the electrophilic capture of sulfoxides, and the addition of sulfonyl radicals to olefins or alkynes. Among them, the selective oxidation of sulfide is a direct method for preparing organic sulfoxide and sulfone.[168] Although a variety of other oxidants such as nitric oxide, different metal oxides, high valence iodine reagents, halides, or high halides, can be used to oxidize sulfides to sulfones, these preparation methods have issues with using toxic reagents, excessive reagent usage, low chemical selectivity or utilizing hazardous organic solvents. With people's attention to the environment, the search for environmentally friendly synthetic methods has been a research hotspot in recent years. In most studies, H_2O_2 is commonly utilized as a "green" oxidant. The oxidation of sulfide to sulfone with H_2O_2 as the oxide is mainly based on metal catalysts.

Trivedi[170] carried out simple and effective sulfonation oxidation with 30% H_2O_2 as oxidant and VCl_3 as a catalyst. Studies have proved that tetrahydrofuran (THF) is a suitable solvent for selective oxidation of sulfide. When the solvent is THF, the sulfide yield is 83–98%.

Jain *et al.*[171] selected diphenyl sulfide as the substrate, 30% H_2O_2 as the oxidant, and Nafion NR-50 as the catalyst to study its oxidation performance, optimize reaction conditions, and select solvent system. The results showed that dichloroethane was the most suitable solvent for the reaction when the catalyst loading was 0.25 g $mmol^{-1}$. When the reaction time was 35 min, the yield was 98%. Jain *et al.* also studied the effect of catalyst loading by using different amounts of Nafion NR-50. It was found that when the catalyst loading was increased from 0.05 to 0.25 g $mmol^{-1}$, the oxidation of diphenyl sulfide would significantly reduce the reaction time. Přech and other coworkers[172] studied the oxidation of *p*-methyl phenyl sulfide (MPS) over layered titanium silicate catalysts with MFI and UTL-derived topology with H_2O_2 as the oxidant. The results indicated that 95% selectivity of methyl phenyl sulfoxide with 40% conversion was achieved using the Ti-IPC-1-Pi catalyst. The selectivity for the oxidation of methyl phenyl sulfide to methyl phenyl sulfoxide is driven by diffusion restriction in the catalyst.

K. Bahrami *et al.*[173] studied the effects of catalyst dosage, H_2O_2 dosage, solvent, and temperature on the catalytic oxidation of sulfide with 30% H_2O_2 as the oxidant and BNPs-SiO_2@$(CH_2)_3NHSO_3H$ as the catalyst. The results show that ethanol is the most suitable solvent for the reaction, and the reaction yield in ethanol solvent is 98%. When the molar ratio between sulfide and H_2O_2 was 1/3, and 0.07 g BNPs-SiO_2@$(CH_2)_3NHSO_3H$ reacted for 10 minutes, the yield was 98%.

10 Conclusions and future perspectives

The utilization of *in situ*-generated H_2O_2 from H_2 and O_2 for selective oxidation presents a promising alternative to current industrial methods. This approach offers mild, eco-friendly reaction conditions, ensuring better control over the process while circumventing the by-products from high-temperature self-oxidation. Contrastingly, utilizing abundant molecular oxygen as a raw material eliminates the need to stockpile large quantities of H_2O_2 on-site, effectively reducing production and equipment costs while sidestepping losses due to commercial H_2O_2 decomposition. However, a key challenge arises from the inherently low yield of directly synthesized H_2O_2 in the absence of stabilizers. The addition of stabilizers tends to influence the overall yield of H_2O_2 while significantly impacting the longevity of catalysts and equipment. In particular, the introduction of stabilizers, such as acids and halogens, can compromise the operational lifespan of both the catalyst and the equipment. Overcoming these scientific hurdles is imperative for advancing synthesis reactions. Moreover, this method entails a dual-reaction process: H_2O_2 synthesis and target substrate oxidation, involving a complex micro mechanism encompassing adsorption, desorption, and diffusion at the active site. Addressing H_2O_2 decomposition is equally pivotal.

Therefore, future catalyst design should prioritize active sites capable of simultaneous dual reactions to minimize diffusion limitations on the generated H_2O_2. It has been proved that the integrated system generates many hydroperoxides and reactive oxygen species *in situ*, promoting the oxidation of inactive C–H bonds to corresponding oxygen-containing compounds. This observed enhancement surpasses the effects achieved by the direct addition of H_2O_2. It can be popularized and designed according to similar strategies, and can deepen the understanding of reaction mechanism, formulate different strategies, improve the overall product yield and realize the economic feasibility of the process route utilizing catalyst design, process parameters, and system control. In addition, enhancing the stability of the catalyst in the selective oxidation process, mitigating metal component loss or poisoning, considering the safety of the reaction system, and controlling the H_2/O_2 mixture ratio in the system are the keys to achieve future industrial applications.

Moreover, electrocatalysis, photocatalysis, and similar methodologies are gaining prominence for their capability to generate H_2O_2 *in situ* under milder conditions. These approaches hold promise as potentially milder and greener reaction pathways for the future. New catalyst designs, including perovskite-type catalysts and the integration of novel porous materials such as COFs, offer promising avenues for oxidation reactions coupled with *in situ* H_2O_2 processes.

Data availability

No primary research results, software or code have been included, and no new data were generated or analysed as part of this review.

Author contributions

All authors have made substantial contributions to the conception, design, investigation, data analysis, or interpretation of this work and have approved the final version of the manuscript. Conceptualization: Jinghui Lyu, Xiaonian Li, and Chengrong Ding; methodology: Han Wu, Qingqing Li, and Shihao Wang; investigation: Jinke Yao, Tao Liu, Wenying Chu, and Feng Feng; data curation and analysis: Qunfeng Zhang, Qingtao Wang, and Dahao Jiang; writing – original draft preparation: Han Wu and Jinghui Lyu; writing – review and editing: Chengrong Ding, Xiaonian Li, and Guofu Zhang; funding acquisition: Xiaonian Li; supervision: Jinghui Lyu, Chengrong Ding, and Xiaonian Li; project administration: Chengrong Ding and Xiaonian Li.

All authors have read and agreed to the published version of the manuscript.

Conflicts of interest

There are no conflicts to declare.

Acknowledgements

This work was supported by the National Natural Science Foundation of China (NSFC22278368 and NSFC21506189), Zhejiang Provincial Natural Science Foundation (No. LY21B060006), the Technology Transfer Project between Zhejiang University of Technology and Industry (Grant No. KYY-ZH-20240069) and the Energy Revolution S&T Program of Yulin Innovation Institute of Clean Energy (Grant No. E412022701).

References

1 Z. Qi, X. F. Wu, Q. Li, C. S. Lu, S. A. C. Carabineiro, Z. W. Zhao, Y. Liu and K. L. Lv, Singlet oxygen in environmental catalysis: Mechanisms, applications and future directions, *Coord. Chem. Rev.*, 2025, **529**, 216439.

2 I. Ali, K. Van Eyck, S. De Laet and R. Dewil, Recent advances in carbonaceous catalyst design for the in situ production of H_2O_2 via two-electron oxygen reduction, *Chemosphere*, 2022, **308**, 136127.

3 A. Byeon, W. C. Yun, J. M. Kim and J. W. Lee, Non-precious metal catalysts for two-electron oxygen reduction reaction, *ChemElectroChem*, 2023, **10**, e202300234.

4 K. Wang, J. Huang, H. Chen, Y. Wang and S. Song, Recent advances in electrochemical 2e oxygen reduction reaction for on-site hydrogen peroxide production and beyond, *Chem. Commun.*, 2020, **56**, 12109–12121.

5 K. Fuku, R. Takioka, K. Iwamura, M. Todoroki, K. Sayama and N. Ikenaga, Photocatalytic H_2O_2 production from O_2 under visible light irradiation over phosphate ion-coated Pd nanoparticles-supported $BiVO_4$, *Appl. Catal., B*, 2020, **272**, 119003.

6 P. Garcia-Munoz, L. Valenzuela, D. Wegstein, T. Schanz, G. E. Lopez, A. M. Ruppert, H. Remita, J. Z. Bloh and N. Keller, Photocatalytic synthesis of hydrogen peroxide from molecular oxygen and water, *Top. Curr. Chem.*, 2023, **381**, 15.

7 L. Li, B. Li, L. Feng, X. Zhang, Y. Zhang, Q. Zhao, G. Zuo and X. Meng, Au modified F-TiO_2 for efficient photocatalytic synthesis of hydrogen peroxide, *Molecules*, 2021, **26**, 3844.

8 J. Lyu, L. Niu, F. Shen, J. Wei, Y. Xiang, Z. Yu, G. Zhang, C. Ding, Y. Huang and X. Li, In situ hydrogen peroxide production for selective oxidation of benzyl alcohol over a Pd@hierarchical titanium silicalite catalyst, *ACS Omega*, 2020, **5**, 16865–16874.

9 J. Lyu, J. Wei, L. Niu, C. Lu, Y. Hu, Y. Xiang, G. Zhang, Q. Zhang, C. Ding and X. Li, Highly efficient hydrogen peroxide direct synthesis over a hierarchical TS-1 encapsulated subnano Pd/PdO hybrid, *RSC Adv.*, 2019, **9**, 13398–13402.

10 N. Mano and A. de Poulpiquet, O_2 reduction in enzymatic biofuel cells, *Chem. Rev.*, 2018, **118**, 2392–2468.

11 C. Leger and P. Bertrand, Direct electrochemistry of redox enzymes as a tool for mechanistic studies, *Chem. Rev.*, 2008, **108**, 2379–2438.

12 J. K. Edwards, B. Solsona, E. N. N, A. F. Carley, A. A. Herzing, C. J. Kiely and G. J. Hutchings, Switching off hydrogen peroxide hydrogenation in the direct synthesis process, *Science*, 2009, **323**, 1037–1041.

13 J. Gu, S. Wang, Z. He, Y. Han and J. Zhang, Direct synthesis of hydrogen peroxide from hydrogen and oxygen over activated-carbon-supported Pd–Ag alloy catalysts, *Catal. Sci. Technol.*, 2016, **6**, 809–817.

14 Y. Liu, G. Chen and J. Yue, Manipulation of gas-liquid-liquid systems in continuous flow microreactors for efficient reaction processes, *J. Flow Chem.*, 2020, **10**, 103–121.

15 V. R. Choudhary, C. Samanta and T. V. Choudhary, Direct oxidation of H_2 to H_2O_2 over Pd-based catalysts: Influence of oxidation state, support and metal additives, *Appl. Catal., A*, 2006, **308**, 128–133.

16 Y. Wang, Y. Wang, B. Hu, M. Qiu, G. Gao and P. Wei, Catalyst-free contact-electro-catalytic H_2O_2 synthesis via simple combination of a poly(tetrafluoroethylene) stir bar and ultrasound, *Chem. Commun.*, 2024, **60**, 7331–7334.

17 J. C. Zhou, J. X. Gou, L. X. Chen, H. C. Guo and X. S. Wang, Direct synthesis of hydrogen peroxide via hydrogen-oxygen plasma, *Chin. J. Chem. Eng.*, 2006, 821–823.

18 J. C. Zhou, Y. H. Yin, H. Y. Zheng, X. Zhou, Y. Xu, J. S. Gong, L. L. Zhang and G. T. Song, Direct synthesis of H_2O_2 using methane-oxygen plasma, *Chem. J. Chin. Univ.*, 2011, **32**, 2240–2242.

19 Y. Shiraishi, S. Kanazawa, Y. Sugano, D. Tsukamoto, H. Sakamoto, S. Ichikawa and T. Hirai, Highly selective production of hydrogen peroxide on graphitic carbon nitride (g-C_3N_4) photocatalyst activated by visible light, *ACS Catal.*, 2014, **4**, 774–780.

20 Y. Kofuji, Y. Isobe, Y. Shiraishi, H. Sakamoto, S. Tanaka, S. Ichikawa and T. Hirai, Carbon nitride-aromatic diimide-graphene nanohybrids: Metal-free photocatalysts for solar-to-hydrogen peroxide energy conversion with 0.2% efficiency, *J. Am. Chem. Soc.*, 2016, **138**, 10019–10025.

21 S. C. Perry, D. Pangotra, L. Vieira, L.-I. Csepei, V. Sieber, L. Wang, C. Ponce de León and F. C. Walsh, Electrochemical synthesis of hydrogen peroxide from water and oxygen, *Nat. Rev. Chem.*, 2019, **3**, 442–458.

22 J. M. Campos-Martin, G. Blanco-Brieva and J. L. Fierro, Hydrogen peroxide synthesis: An outlook beyond the anthraquinone process, *Angew. Chem., Int. Ed.*, 2006, **45**, 6962–6984.

23 S. Siahrostami, A. Verdaguer-Casadevall, M. Karamad, D. Deiana, P. Malacrida, B. Wickman, M. Escudero-Escribano, E. A. Paoli, R. Frydendal, T. W. Hansen, I. Chorkendorff, I. E. Stephens and J. Rossmeisl, Enabling direct H_2O_2 production through rational electrocatalyst design, *Nat. Mater.*, 2013, **12**, 1137–1143.

24 L. Han, Y. Sun, S. Li, C. Cheng, C. E. Halbig, P. Feicht, J. L. Hübner, P. Strasser and S. Eigler, In-plane carbon lattice-

defect regulating electrochemical oxygen reduction to hydrogen peroxide production over nitrogen-doped graphene, *ACS Catal.*, 2019, **9**, 1283–1288.

25 E. Jung, H. Shin, B. H. Lee, V. Efremov, S. Lee, H. S. Lee, J. Kim, W. Hooch Antink, S. Park, K. S. Lee, S. P. Cho, J. S. Yoo, Y. E. Sung and T. Hyeon, Atomic-level tuning of Co-N-C catalyst for high-performance electrochemical H_2O_2 production, *Nat. Mater.*, 2020, **19**, 436–442.

26 Y. Sun, L. Silvioli, N. R. Sahraie, W. Ju, J. Li, A. Zitolo, S. Li, A. Bagger, L. Arnarson, X. Wang, T. Moeller, D. Bernsmeier, J. Rossmeisl, F. Jaouen and P. Strasser, Activity-selectivity trends in the electrochemical production of hydrogen peroxide over single-site metal-nitrogen-carbon catalysts, *J. Am. Chem. Soc.*, 2019, **141**, 12372–12381.

27 Z. Jin, M. Lu, C. Jiang, S. Wu, L. Tang, C. Hu, L. Liu, L. Fang and Z. Cheng, Mechanocatalytic H_2O_2 production using ferroelectric $KSr_2Nb_3Ta_2O_{15}$ nanorods, *Nano Energy*, 2025, **138**, 110892.

28 J. Ji, Z. Lu, Y. Lei and C. H. Turner, Theoretical studies on the direct propylene epoxidation using gold-based catalysts: A mini-review, *Catalysts*, 2018, **8**, 421.

29 N. Kapil, T. Weissenberger, F. Cardinale, P. Trogadas, T. A. Nijhuis, M. M. Nigra and M.-O. Coppens, Precisely engineered supported gold clusters as a stable catalyst for propylene epoxidation, *Angew. Chem., Int. Ed.*, 2021, **60**, 18185–18193.

30 K. Dong, Y. Wang, L. Zhang, X. Fan, Z. Li, D. Zhao, L. Yue, S. Sun, Y. Luo, Q. Liu, A. A. Alshehri, Q. Li, D. Ma and X. Sun, Epoxidation of olefins enabled by an electro-organic system, *Green Chem.*, 2022, **24**, 8264–8269.

31 X. Wang, P. Zhou, Q. Zhou, Q. Zhang, H. Ning, M. Wu and W. Wu, Tandem photocatalytic production of H_2O_2 and propylene oxide on 5-Bro- moisatin modified carbon nitride, *Chem. Eng. J.*, 2023, **476**, 146488.

32 M. Ko, Y. Kim, J. Woo, B. Lee, R. Mehrotra, P. Sharma, J. Kim, S. W. Hwang, H. Y. Jeong, H. Lim, S. H. Joo, J.-W. Jang and J. H. Kwak, Direct propylene epoxidation with oxygen using a photo-electro-heterogeneous catalytic system, *Nat. Catal.*, 2022, **5**, 37–44.

33 Y. Liu, C. Zhao, B. Sun, H. Zhu and W. Xu, Preparation and modification of Au/TS-1 catalyst in the direct epoxidation of propylene with H_2 and O_2, *Appl. Catal., A*, 2021, **624**, 118329.

34 J. García-Aguilar, J. Fernández-Catalá, J. Juan-Juan, I. Such-Basáñez, L. E. Chinchilla, J. J. Calvino-Gámez, D. Cazorla-Amorós and Á. Berenguer-Murcia, Novelty without nobility: Outstanding Ni/Ti-SiO_2 catalysts for propylene epoxidation, *J. Catal.*, 2020, **386**, 94–105.

35 W. Li, L. Chen, M. Qiu, W. Li, Y. Zhang, Y. Zhu, J. Li and X. Chen, Highly efficient epoxidation of propylene with in situ-generated H_2O_2 over a hierarchical TS-1 zeolite-supported non-noble nickel catalyst, *ACS Catal.*, 2023, **13**, 10487–10499.

36 Y. Zheng, M. Okumura, X. Hua, A. Sonoura, H. Su, H. Nobutou, X. Sun, L. Sun, F. Xiao and C. Qi, Partial oxidation of propylene with H_2 and O_2 over Au supported on ZrO_2 with different structural and surface properties, *J. Catal.*, 2021, **401**, 188–199.

37 T. Ishida, T. Murayama, A. Taketoshi and M. Haruta, Importance of size and contact structure of gold nanoparticles for the genesis of unique catalytic processes, *Chem. Rev.*, 2020, **120**, 464–525.

38 F. X. Song Zhaoning, Liu Yibin, Yang Chaohe and Zhou Xinggui, Advances in manipulation of catalyst structure and relationship of structure-performance for direct propene epoxidation with H_2 and O_2, *Prog. Chem.*, 2016, **28**, 1762–1773.

39 Z. Li, J. Zhang, D. Wang, W. Ma and Q. Zhong, Confirmation of gold active sites on titanium-silicalite-1-supported nano-gold catalysts for gas-phase epoxidation of propylene, *J. Phys. Chem. C*, 2017, **121**, 25215–25222.

40 F. Jin, Y. Wu, S. Liu, T.-H. Lin, J.-F. Lee and S. Cheng, Effect of Ti incorporated MWW supports on Au loading and catalytic performance for direct propylene epoxidation, *Catal. Today*, 2016, **264**, 98–108.

41 X. Feng, D. Chen and X. G. Zhou, Thermal stability of TPA template and size-dependent selectivity of uncalcined TS-1 supported Au catalyst for propene epoxidation with H_2 and O_2, *RSC Adv.*, 2016, **6**, 44050–44056.

42 C. Zhuang, Y. Chang, W. Li, S. Li, P. Xu, H. Zhang, Y. Zhang, C. Zhang, J. Gao, G. Chen, T. Zhang, Z. Kang and X. Han, Light-induced variation of lithium coordination environment in g-C_3N_4 nanosheet for highly efficient oxygen reduction reactions, *ACS Nano*, 2024, **18**, 5206–5217.

43 S. Chen, D. Li, T. Cao and W. Huang, Size-dependent structures and catalytic performances of Au/TiO_2-{001} catalysts for propene epoxidation, *J. Phys. Chem. C*, 2020, **124**, 15264–15274.

44 Q. J. Zhang, C. Yao, F. Zhang, Y. C. Chen, Z. L. Li, Y. K. Zhou, Y. X. Qin, L. Y. Xu, F. Feng, J. Zhao, C. S. Lu, Q. F. Zhang, Q. T. Wang and X. N. Li, Constructing oxygen vacancies in anatase TiO_2: Enhancing acetylene semi-hydrogenation performance through H_2 heterolytic cleavage, *J. Mater. Chem. A*, 2025, **13**, 5180–5190.

45 Y. Hong, L. Ke, Z. Li, J. Huang, G. Zhan, Y. Zhou, D. Sun, J. Zhang and Q. Li, Seed-induced zeolitic TS-1 immobilized with bioinspired-Au nanoparticles for propylene epoxidation with O_2 and H_2, *Catal. Lett.*, 2020, **150**, 1798–1811.

46 Z. Su, L. Gao, J. Gao and W. Ma, Effect of nickel promoter in Au/TS-1 catalysts for gas-phase propylene epoxidation, *J. Porous Mater.*, 2022, **29**, 143–152.

47 J. Peng, K. Liu, S. Guo, W. Chen, H. Hu, Q. Huang and X. Chen, Synthesis strategy of atomically dispersed Au clusters induced by NH_3 on TS-1: Significantly improve the epoxidation activity of propylene, *Chem. Eng. J.*, 2023, **472**, 144895.

48 S. Yao, L. Xu, J. Wang, X. Jing, T. Odoom-Wubah, D. Sun, J. Huang and Q. Li, Activity and stability of titanosilicate supported Au catalyst for propylene epoxidation with H_2 and O_2, *Mol. Catal.*, 2018, **448**, 144–152.

49 X. Feng, Z. Song, Y. Liu, X. Chen, X. Jin, W. Yan, C. Yang, J. Luo, X. Zhou and D. Chen, Manipulating gold spatial location on titanium silicalite-1 to enhance the catalytic performance for direct propene epoxidation with H_2 and O_2, *ACS Catal.*, 2018, **8**, 10649–10657.

50 X. Feng, Y. Liu, Y. Li, C. Yang, Z. Zhang, X. Duan, X. Zhou and D. Chen, Au/TS-1 catalyst for propene epoxidation with H_2/O_2: A novel strategy to enhance stability by tuning charging sequence, *AIChE J.*, 2016, **62**, 3963–3972.

51 X. Li, A. Gao, Z. Wan, Q. Huang and X. Chen, The construction of Au–Fe–TS-1 interface coupling structure for improving catalytic performance of propylene epoxidation with H_2 and O_2, *Catal. Lett.*, 2020, **150**, 3149–3158.

52 X. Feng, J. Yang, X. Duan, Y. Cao, B. Chen, W. Chen, D. Lin, G. Qian, D. Chen, C. Yang and X. Zhou, Enhanced catalytic performance for propene epoxidation with H_2 and O_2 over bimetallic Au–Ag/uncalcined titanium silicate-1 catalysts, *ACS Catal.*, 2018, **8**, 7799–7808.

53 Z. Li, L. Gao, W. Ma and Q. Zhong, Higher gold atom efficiency over Au-Pd/TS-1 alloy catalysts for the direct propylene epoxidation with H_2 and O_2, *Appl. Surf. Sci.*, 2019, **497**, 143749.

54 Z. Li, L. Gao, X. Zhu, W. Ma, X. Feng and Q. Zhong, Synergistic enhancement over Au-Pd/TS-1 bimetallic catalysts for propylene epoxidation with H_2 and O_2, *ChemCatChem*, 2019, **11**, 5116–5123.

55 J. Qiu, K. Meng, Y. Zhang, B. Cheng, J. Zhang, L. Wang and J. Yu, COF/In_2S_3 S-scheme photocatalyst with enhanced light absorption and H_2O_2-production activity and fs-TA investigation, *Adv. Mater.*, 2024, **36**, 288.

56 Q. Zhu, M. Liang, W. Yan and W. Ma, Effective hierarchization of TS-1 and its catalytic performance in propene epoxidation, *Microporous Mesoporous Mater.*, 2019, **278**, 307–313.

57 X. Feng, N. Sheng, Y. Liu, X. Chen, D. Chen, C. Yang and X. Zhou, Simultaneously enhanced stability and selectivity for propene epoxidation with H_2 and O_2 on Au catalysts supported on nano-crystalline mesoporous TS-1, *ACS Catal.*, 2017, **7**, 2668–2675.

58 Z. Song, X. Feng, N. Sheng, D. Lin, Y. Li, Y. Liu, X. Chen, X. Zhou, D. Chen and C. Yang, Propene epoxidation with H_2 and O_2 on Au/TS-1 catalyst: Cost-effective synthesis of small-sized mesoporous TS-1 and its unique performance, *Catal. Today*, 2020, **347**, 102–109.

59 J. Yuan, Z. Song, D. Lin, X. Feng, Y. Tuo, X. Zhou, H. Yan, X. Jin, Y. Liu, X. Chen, D. Chen and C. Yang, Mesoporogen-free strategy to construct hierarchical TS-1 in a highly concentrated system for gas-phase propene epoxidation with H_2 and O_2, *ACS Appl. Mater. Interfaces*, 2021, **13**, 26134–26142.

60 N. Sheng, Z. Liu, Z. Song, D. Lin, X. Feng, Y. Liu, X. Chen, D. Chen, X. Zhou and C. Yang, Enhanced stability for propene epoxidation with H_2 and O_2 over wormhole-like hierarchical TS-1 supported Au nanocatalyst, *Chem. Eng. J.*, 2019, **377**, 119954.

61 C. Zhuang, W. Li, Y. Chang, S. Li, Y. Zhang, Y. Li, J. Gao, G. Chen and Z. Kang, Coordination environment dominated catalytic selectivity of photocatalytic hydrogen and oxygen reduction over switchable gallium and nitrogen active sites, *J. Mater. Chem. A*, 2024, **12**, 5711–5718.

62 C. Ma, X. Xu, M. Xu, Y. Zhou, Y. Yao, Z. Xiang, W. He, J. Yu, Q. Zhang, F. Feng, Y. Liu, C. Yin, X. Li and C. Lu, NCQD-induced nitrogen configuration engineering for constructing hybrid CN with exceptionally high nitrogen content and predominantly pyrrolic/pyridinic-N for catalytic hydrogenation, *J. Mater. Chem. A*, 2025, **13**, 12507–12522.

63 Z. Li, W. Ma and Q. Zhong, Effect of core–shell support on Au/S-1/TS-1 for direct propylene epoxidation and design of catalyst with higher activity, *Ind. Eng. Chem. Res.*, 2019, **58**, 4010–4016.

64 Z. Song, X. Feng, N. Sheng, D. Lin, Y. Li, Y. Liu, X. Chen, D. Chen, X. Zhou and C. Yang, Cost-efficient core-shell TS-1/silicalite-1 supported Au catalysts: Towards enhanced stability for propene epoxidation with H_2 and O_2, *Chem. Eng. J.*, 2019, **377**, 119927.

65 Z. Li, W. Ma and Q. Zhong, Insight into deactivation reasons for nanogold catalysts used in gas-phase epoxidation of propylene, *Catal. Lett.*, 2020, **150**, 1856–1864.

66 L. Wang, J. Dai, Y. Xu, Y. Hong, J. Huang, D. Sun and Q. Li, Titanium silicalite-1 zeolite encapsulating Au particles as a catalyst for vapor phase propylene epoxidation with H_2/O_2: A matter of Au–Ti synergic interaction, *J. Mater. Chem. A*, 2020, **8**, 4428–4436.

67 Z. Song, J. Yuan, Z. Cai, D. Lin, X. Feng, N. Sheng, Y. Liu, X. Chen, X. Jin, D. Chen and C. Yang, Engineering three-layer core–shell S-1/TS-1@dendritic-SiO_2 supported Au catalysts towards improved performance for propene epoxidation with H_2 and O_2, *Green Energy Environ.*, 2020, **5**, 473–483.

68 S. Kanungo, K. S. Keshri, E. J. M. Hensen, B. Chowdhury, J. C. Schouten and M. F. Neira d'Angelo, Direct epoxidation of propene on silylated Au–Ti catalysts: A study on silylation procedures and the effect on propane formation, *Catal. Sci. Technol.*, 2018, **8**, 3052–3059.

69 E. J. J. de Boed, J. W. de Rijk, P. E. de Jongh and B. Donoeva, Steering the selectivity in gold–titanium-catalyzed propene oxidation by controlling the surface acidity, *J. Phys. Chem. C*, 2021, **125**, 16557–16568.

70 Z. Lu, X. Liu, B. Zhang, Z. Gan, S. Tang, L. Ma, T. Wu, G. J. Nelson, Y. Qin, C. H. Turner and Y. Lei, Structure and reactivity of single site Ti catalysts for propylene epoxidation, *J. Catal.*, 2019, **377**, 419–428.

71 Z. Lu, J. Kunisch, Z. Gan, M. Bunian, T. Wu and Y. Lei, Gold catalysts synthesized using a modified incipient wetness impregnation method for propylene epoxidation, *ChemCatChem*, 2020, **12**, 5993–5999.

72 Z. Li, Y. Wang, J. Zhang, D. Wang and W. Ma, Better performance for gas-phase epoxidation of propylene using H_2 and O_2 at lower temperature over Au/TS-1 catalyst, *Catal. Commun.*, 2017, **90**, 87–90.

73 N. Li, Y. Chen, Q. Shen, B. Yang, M. Liu, L. Wei, W. Tian and J. Zhou, TS-1 supported highly dispersed sub-5 nm gold

nanoparticles toward direct propylene epoxidation using H_2 and O_2, *J. Solid State Chem.*, 2018, **261**, 92–102.

74 Y.-G. Ren, J. Huang, Q. Lv, Y. Xie, A.-H. Lu and M. Haruta, Dual-component gas pretreatment for Au/TS-1: Enhanced propylene epoxidation with oxygen and hydrogen, *Appl. Catal., A*, 2019, **584**, 117172.

75 J. Xu, Z. Zhang, G. Wang, X. Duan, G. Qian and X. Zhou, Zeolite crystal size effects of Au/uncalcined TS-1 bifunctional catalysts on direct propylene epoxidation with H_2 and O_2, *Chem. Eng. Sci.*, 2020, **227**, 115907.

76 Y. Hong, J. Huang, G. Zhan and Q. Li, Biomass-modified Au/TS-1 as highly efficient and stable nanocatalysts for propene epoxidation with O_2 and H_2, *Ind. Eng. Chem. Res.*, 2019, **58**, 21953–21960.

77 G. Wang, Y. Cao, Z. Zhang, J. Xu, M. Lu, G. Qian, X. Duan, W. Yuan and X. Zhou, Surface engineering and kinetics behaviors of Au/uncalcined TS-1 catalysts for propylene epoxidation with H_2 and O_2, *Ind. Eng. Chem. Res.*, 2019, **58**, 17300–17307.

78 G. Wang, W. Du, Z. Zhang, Y. Tang, J. Xu, Y. Cao, G. Qian, X. Duan, W. Yuan and X. Zhou, Combining trace Pt with surface silylation to boost Au/uncalcined TS-1 catalyzed propylene epoxidation with H_2 and O_2, *AIChE J.*, 2022, **68**, e17416.

79 T. Lian, W. Zeng, H. Liu, J. Yu, J. Huang, H. Wang and D. Sun, The influence of active biomolecules in plant extracts on the performance of Au/TS-1 catalysts in propylene epoxidation, *Eur. J. Inorg. Chem.*, 2019, **2019**, 2853–2859.

80 Y. Ren, X. Sun, J. Huang, L. Zhang, B. Zhang, M. Haruta and A.-H. Lu, Dual-component sodium and cesium promoters for Au/TS-1: Enhancement of propene epoxidation with hydrogen and oxygen, *Ind. Eng. Chem. Res.*, 2020, **59**, 8155–8163.

81 T. Ayvalı, L. Ye, S. Wu, B. T. W. Lo, C. Huang, B. Yu, G. Cibin, A. I. Kirkland, C. Tang, A. A. Bagabas and S. C. E. Tsang, Mononuclear gold species anchored on TS-1 framework as catalyst precursor for selective epoxidation of propylene, *J. Catal.*, 2018, **367**, 229–233.

82 Z. Zhang, X. Zhao, G. Wang, J. Xu, M. Lu, Y. Tang, W. Fu, X. Duan, G. Qian, D. Chen and X. Zhou, Uncalcined TS-2 immobilized Au nanoparticles as a bifunctional catalyst to boost direct propylene epoxidation with H_2 and O_2, *AIChE J.*, 2020, **66**, e16815.

83 J. Gao, L. Gao, B. Zhang, H. Wang and W. Ma, Synthesis of titanium silicalite-1 with high titanium content and its catalytic performance of propylene epoxidation, *Can. J. Chem. Eng.*, 2021, **99**, S596–S604.

84 Z. Li, X. Chen, W. Ma and Q. Zhong, Effect of TS-1 crystal planes on the catalytic activity of Au/TS-1 for direct propylene epoxidation with H_2 and O_2, *ACS Sustainable Chem. Eng.*, 2020, **8**, 8496–8504.

85 D. Lin, Q. Zhang, Z. Qin, Q. Li, X. Feng, Z. Song, Z. Cai, Y. Liu, X. Chen, D. Chen, S. Mintova and C. Yang, Reversing titanium oligomer formation towards high-efficiency and green synthesis of titanium-containing molecular sieves, *Angew. Chem., Int. Ed.*, 2021, **60**, 3443–3448.

86 Z. Lu, M. Piernavieja-Hermida, C. H. Turner, Z. Wu and Y. Lei, Effects of TiO_2 in low temperature propylene epoxidation using gold catalysts, *J. Phys. Chem. C*, 2018, **122**, 1688–1698.

87 Y. Y. Sun, W. Zhao, W. Cai, Y. H. Chi, H. Ren and Z. T. Li, Single-atom M/GDY catalysts for electrochemical ethylene conversion via tandem water oxidation, *Appl. Surf. Sci.*, 2025, **695**, 162865.

88 T. C. Pu, H. J. Tian, M. E. Ford, S. Rangarajan and I. E. Wachs, Overview of selective oxidation of ethylene to ethylene oxide by ag catalysts, *ACS Catal.*, 2019, **9**, 10727–10750.

89 A. Z. Li, B. J. Yuan, M. Xu, Y. Wang, C. Y. Zhang, X. B. Wang, X. Wang, J. Li, L. R. Zheng, B. J. Li and H. H. Duan, One-step electrochemical ethylene-to-ethylene glycol conversion over a multitasking molecular catalyst, *J. Am. Chem. Soc.*, 2024, **146**, 5622–5633.

90 D. Li and H. Wang, Market and technology progress of syngas to ethylene glycol, *Xiandai Huagong*, 2017, **37**, 5.

91 H. L. Tan, Y. Zuo, G. D. Li, B. S. Zhang, L. A. Li, L. L. Guo, J. R. Zeng, F. Song, H. Yang and X. W. Guo, A titanium silicalite-1 (TS-1) catalyst with abundant active Ti-VI species for efficient conversion of ethylene to glycol, *Angew. Chem.*, 2025, **64**, 02003.

92 J. E. Yoon, K. B. Lee, C. J. Yoo, B. K. Min, D. K. Lee, D. H. Won, S. Kim, J. H. Moon, C. Kim and U. Lee, Investigation of the sustainable production of ethylene oxide by electrochemical conversion: Techno-economic assessment and CO_2 emissions, *J. Cleaner Prod.*, 2024, **475**, 143539.

93 L. Fan, Y. L. Zhao, L. Chen, J. Y. Chen, J. M. Chen, H. Z. Yang, Y. K. Xiao, T. Y. Zhang, J. Y. Chen and L. Wang, Selective production of ethylene glycol at high rate via cascade catalysis, *Nat. Catal.*, 2023, **6**, 585–595.

94 M. H. Guan, L. Y. Dong, T. Wu, W. C. Li, G. P. Hao and A. H. Lu, Boosting selective oxidation of ethylene to ethylene glycol assisted by in situ generated H_2O_2 from O_2 electroreduction, *Angew. Chem., Int. Ed.*, 2023, **62**, 02466.

95 H. Z. Yang, N. Guo, S. B. Xi, J. X. Yin, T. Song, Y. K. Xiao, L. L. Duan, C. Zhang and L. Wang, Scalable H_2O_2 production via O_2 reduction using immobilized vanadyl phthalocyanine, *Angew. Chem., Int. Ed.*, 2025, e09079.

96 J. Droenner, P. Hausoul, R. Palkovits and M. Eisenacher, Solid acid catalysts for the Hock cleavage of hydroperoxides, *Catalysts*, 2022, **12**, 9.

97 X. Wang, Y. Zou, B. Meng, X. Tan, S. Wang and S. Liu, Catalytic palladium membrane reactors for one-step benzene hydroxylation to phenol, *J. Membr. Sci.*, 2018, **563**, 864–872.

98 J. H. Masakazu Iwamoto, Kazuto Matsukami and Shuichi Kagawa, Catalytic oxidation by oxide radical ions. 1. one-step hydroxylation of benzene to phenol over group 5 and 6 oxldes supported on silica gel, *J. Phys. Chem.*, 1983, **87**, 903–905.

99 T. Ren, L. Yan, H. Zhang and J. Suo, Study on Fe-P-O based catalysts in the gas-phase direct oxidation of benzene to

phenol with N_2O as an oxidant, *J. Mol. Catal.*, 2003, **17**, 342–346.

100 R. Leanza, I. Rossetti, I. Mazzola and L. Forni, Study of Fe-silicalite catalyst for the N_2O oxidation of benzene to phenol, *Appl. Catal., A*, 2001, **205**, 93–99.

101 Y. Leng, H. Ge, C. Zhou and J. Wang, Direct hydroxylation of benzene with hydrogen peroxide over pyridine-heteropoly compounds, *Chem. Eng. J.*, 2008, **145**, 335–339.

102 J. Zhang, Y. Tang, G. Y. Li and C. Hu, Room temperature direct oxidation of benzene to phenol using hydrogen peroxide in the presence of vanadium-substituted heteropolymolybdates, *Appl. Catal., A*, 2005, **278**, 251–261.

103 H. H. Monfared and Z. Amouei, Hydrogen peroxide oxidation of aromatic hydrocarbons by immobilized iron(III), *J. Mol. Catal. A:Chem.*, 2004, **217**, 161–164.

104 K. Sato, T. A. Hanaoka, S. Niwa, C. Stefan, T. Namba and F. Mizukami, Direct hydroxylation of aromatic compounds by a palladium membrane reactor, *Catal. Today*, 2005, **104**, 260–266.

105 S.-I. Niwa, M. Eswaramoorthy, J. Nair, A. Raj, N. Itoh, H. Shoji, T. Namba and F. Mizukami, A one-step conversion of benzene to phenol with a palladium membrane, *Science*, 2002, **295**, 105–107.

106 X. Wang, X. Zhang, H. Liu, J. Qiu, W. Han and K. L. Yeung, Investigation of Pd membrane reactors for one-step hydroxylation of benzene to phenol, *Catal. Today*, 2012, **193**, 151–157.

107 N. Itoh, S. Niwa, F. Mizukami, T. Inoue, A. Igarashi and T. Namba, Catalytic palladium membrane for reductive oxidation of benzene to phenol, *Catal. Commun.*, 2003, **4**, 243–246.

108 Y. Y. Zhao, J. Y. Sun, J. X. Miao, X. H. Zhang, H. Wu, Q. F. Zhang, Y. W. Peng, C. R. Ding, J. Lyu and X. N. Li, Insight into the mechanism of semi-hydrogenation of phenylacetylene over Pd embedded in thioether functionalized schiff-base linked covalent organic frameworks, *Chem. Commun.*, 2025, **61**, 5822–5825.

109 R. Dittmeyer and L. Bortolotto, Modification of the catalytic properties of a Pd membrane catalyst for direct hydroxylation of benzene to phenol in a double-membrane reactor by sputtering of different catalyst systems, *Appl. Catal., A*, 2011, **391**, 311–318.

110 X. Wang, Y. Guo, X. Zhang, Y. Wang, H. Liu, J. Wang, J. Qiu and K. L. Yeung, Catalytic properties of benzene hydroxylation by TS-1 film reactor and Pd-TS-1 composite membrane reactor, *Catal. Today*, 2010, **156**, 288–294.

111 K. Sato, S. Hamakawa, M. Natsui, M. Nishioka, T. Inoue and F. Mizukami, Palladium-based bifunctional membrane reactor for one-step conversion of benzene to phenol and cyclohexanone, *Catal. Today*, 2010, **156**, 276–281.

112 Y. Guo, X. Wang, X. Zhang, Y. Wang, H. Liu, J. Wang, J. Qiu and K. L. Yeung, Pd-silicalite-1 composite membrane reactor for direct hydroxylation of benzene to phenol, *Catal. Today*, 2010, **156**, 282–287.

113 L. Bortolotto and R. Dittmeyer, Direct hydroxylation of benzene to phenol in a novel microstructured membrane reactor with distributed dosing of hydrogen and oxygen, *Sep. Purif. Technol.*, 2010, **73**, 51–58.

114 S. Shu, Y. Huang, X. Hu, Y. Fan and N. Xu, On the membrane reactor concept for one-step hydroxylation of benzene to phenol with oxygen and hydrogen, *J. Phys. Chem. C*, 2009, **113**, 19618–19622.

115 Y. Guo, X. Zhang, H. Zou, H. Liu, J. Wang and K. L. Yeung, Pd-silicalite-1 composite membrane for direct hydroxylation of benzene, *Chem. Commun.*, 2009, 5898–5900.

116 M. H. Sayyar and R. J. Wakeman, Comparing two new routes for benzene hydroxylation, *Chem. Eng. Res. Des.*, 2008, **86**, 517–526.

117 K. Sato, T.-A. Hanaoka, S. Hamakawa, M. Nishioka, K. Kobayashi, T. Inoue, T. Namba and F. Mizukami, Structural changes of a Pd-based membrane during direct hydroxylation of benzene to phenol, *Catal. Today*, 2006, **118**, 57–62.

118 G. D. Vulpescu, M. Ruitenbeek, L. L. van Lieshout, L. A. Correia, D. Meyer and P. Pex, One-step selective oxidation over a Pd-based catalytic membrane; Evaluation of the oxidation of benzene to phenol as a model reaction, *Catal. Commun.*, 2004, **5**, 347–351.

119 X. Zhang, D. Gao, B. Zhu, B. Cheng, J. Yu and H. Yu, Enhancing photocatalytic H_2O_2 production with Au co-catalysts through electronic structure modification, *Nat. Commun.*, 2024, **15**, 7.

120 W. He, Y. Li, Q. Xiang, X. Zhang, J. Yu, C. Ma, Y. Yao, C. Yin, Y. Liu, Y. Zhou, X. Li and C. Lu, Enhancing electron penetration through carbon shell of encapsulated catalysts by Co alloying for aromatic nitrobenzene hydrogenation, *J. Catal.*, 2025, **447**, 116150.

121 W. Liu, X. Wang, R. Zhao, B. Meng, C. Zuo and X. Tan, A Pd-TSH composite membrane reactor for one-step oxidation of benzene to phenol, *Chem. Commun.*, 2019, **55**, 7745–7748.

122 X. Wang, B. Meng, X. Tan, X. Zhang, S. Zhuang and L. Liu, Direct hydroxylation of benzene to phenol using palladium–titanium silicalite zeolite bifunctional membrane reactors, *Ind. Eng. Chem. Res.*, 2014, **53**, 5636–5645.

123 X. Wang, X. Tan, B. Meng, X. Zhang, Q. Liang, H. Pan and S. Liu, One-step hydroxylation of benzene to phenol via a Pd capillary membrane microreactor, *Catal. Sci. Technol.*, 2013, **3**, 2380–2391.

124 B. Han, Y. Yang, Y. Xu, U. J. Etim, K. Qiao, B. Xu and Z. Yan, A review of the direct oxidation of methane to methanol, *Chin. J. Catal.*, 2016, **37**, 1206–1215.

125 M. S. A. Sher Shah, C. Oh, H. Park, Y. J. Hwang, M. Ma and J. H. Park, Catalytic oxidation of methane to oxygenated products: Recent advancements and prospects for electrocatalytic and photocatalytic conversion at low temperatures, *Adv. Sci.*, 2020, **7**, 2001946.

126 A. R. Kulkarni, Z.-J. Zhao, S. Siahrostami, J. K. Nørskov and F. Studt, Cation-exchanged zeolites for the selective oxidation of methane to methanol, *Catal. Sci. Technol.*, 2018, **8**, 114–123.

127 V. L. Sushkevich, D. Palagin, M. Ranocchiari and J. A. van Bokhoven, Selective anaerobic oxidation of methane enables direct synthesis of methanol, *Science*, 2017, **356**, 523–527.

128 Y. Liu, L. Wang and F.-S. Xiao, Selective oxidation of methane into methanol under mild conditions, *Chem. Res. Chin. Univ.*, 2022, **38**, 671–676.

129 N. Agarwal, S. J. Freakley, R. U. McVicker, S. M. Althahban, N. Dimitratos, Q. He, D. J. Morgan, R. L. Jenkins, D. J. Willock, S. H. Taylor, C. J. Kiely and G. J. Hutchings, Aqueous Au-Pd colloids catalyze selective CH_4 oxidation to CH_3OH with O_2 under mild conditions, *Science*, 2017, **358**, 223–227.

130 J. H. Carter, R. J. Lewis, N. Demetriou, C. Williams, T. E. Davies, T. Qin, N. F. Dummer, D. J. Morgan, D. J. Willock, X. Liu, S. H. Taylor and G. J. Hutchings, The selective oxidation of methane to methanol using in situ generated H_2O_2 over palladium-based bimetallic catalysts, *Catal. Sci. Technol.*, 2023, **13**, 5848–5858.

131 F. Ni, T. Richards, L. R. Smith, D. J. Morgan, T. E. Davies, R. J. Lewis and G. J. Hutchings, Selective oxidation of methane to methanol via in situ H_2O_2 synthesis, *ACS Org. Inorg. Au*, 2023, **3**, 177–183.

132 M. H. Ab Rahim, M. M. Forde, C. Hammond, R. L. Jenkins, N. Dimitratos, J. A. Lopez-Sanchez, A. F. Carley, S. H. Taylor, D. J. Willock and G. J. Hutchings, Systematic study of the oxidation of methane using supported gold palladium nanoparticles under mild aqueous conditions, *Top. Catal.*, 2013, **56**, 1843–1857.

133 M. H. Ab Rahim, M. M. Forde, R. L. Jenkins, C. Hammond, Q. He, N. Dimitratos, J. A. Lopez-Sanchez, A. F. Carley, S. H. Taylor, D. J. Willock, D. M. Murphy, C. J. Kiely and G. J. Hutchings, Oxidation of methane to methanol with hydrogen peroxide using supported gold–palladium alloy nanoparticles, *Angew. Chem., Int. Ed.*, 2013, **52**, 1280–1284.

134 M. H. Ab Rahim, R. D. Armstrong, C. Hammond, N. Dimitratos, S. J. Freakley, M. M. Forde, D. J. Morgan, G. Lalev, R. L. Jenkins, J. A. Lopez-Sanchez, S. H. Taylor and G. J. Hutchings, Low temperature selective oxidation of methane to methanol using titania supported gold palladium copper catalysts, *Catal. Sci. Technol.*, 2016, **6**, 3410–3418.

135 Y. He, J. Liang, Y. Imai, K. Ueda, H. Li, X. Guo, G. Yang, Y. Yoneyama and N. Tsubaki, Highly selective synthesis of methanol from methane over carbon materials supported Pd-Au nanoparticles under mild conditions, *Catal. Today*, 2020, **352**, 104–110.

136 Y. He, C. Luan, Y. Fang, X. Feng, X. Peng, G. Yang and N. Tsubaki, Low-temperature direct conversion of methane to methanol over carbon materials supported Pd-Au nanoparticles, *Catal. Today*, 2020, **339**, 48–53.

137 J. Kang and E. D. Park, Aqueous-phase selective oxidation of methane with oxygen over iron salts and Pd/C in the presence of hydrogen, *ChemCatChem*, 2019, **11**, 4247–4251.

138 J. Kang and E. D. Park, Selective oxidation of methane over Fe-zeolites by in situ generated H_2O_2, *Catalysts*, 2020, **10**, 299.

139 J. Kang, P. Puthiaraj, W.-S. Ahn and E. D. Park, Direct synthesis of oxygenates via partial oxidation of methane in the presence of O_2 and H_2 over a combination of Fe-ZSM-5 and Pd supported on an acid-functionalized porous polymer, *Appl. Catal., A*, 2020, **602**, 117711.

140 J. Lyu, X. Zhang, Z. Luo, Y. Jiang, K. Xing, G. Zhang and C. Ding, Thianthrenium salts to arynes: Base promoted C-N bond construction, *Adv. Synth. Catal.*, 2025, **367**, 899.

141 X. Yin, H. Shi, Y. Wang, X. Wang, P. Wang and H. Yu, Spontaneously improved adsorption of H_2O and its intermediates on electron-deficient Mn(3+δ)+ for efficient photocatalytic H_2O_2 production, *Acta Phys.-Chim. Sin.*, 2024, **40**, 12007.

142 Z. Jin, L. Wang, E. Zuidema, K. Mondal, M. Zhang, J. Zhang, C. Wang, X. Meng, H. Yang, C. Mesters and F.-S. Xiao, Hydrophobic zeolite modification for in situ peroxide formation in methane oxidation to methanol, *Science*, 2020, **367**, 193–197.

143 K. Sato, M. Aoki and R. Noyori, A "green" route to adipic acid: Direct oxidation of cyclohexenes with 30 percent hydrogen peroxide, *Science*, 1998, **281**, 1646–1647.

144 A. P. C. Ribeiro, E. Spada, R. Bertani and L. M. D. R. S. Martins, Adipic acid route: Oxidation of cyclohexene vs. cyclohexane, *Catalysts*, 2020, **10**, 121443.

145 S. Van de Vyver and Y. Román-Leshkov, Emerging catalytic processes for the production of adipic acid, *Catal. Sci. Technol.*, 2013, **3**, 1465–1479.

146 R. Noyori, M. Aoki and K. Sato, Green oxidation with aqueous hydrogen peroxide, *Chem. Commun.*, 2003, 1977–1986.

147 W. Zhang, P. Zhang, Q. Yang and K. Li, Research progress of peroxygenase-catalyzed reactions driven by in-situ generation of H_2O_2, *Chin. J. Org. Chem.*, 2022, **42**, 3.

148 S. Jiang, M. Xiao, W. Sun, D. Crespy, V. Mailänder, X. Peng, J. Fan and K. Landfester, Synergistic anticancer therapy by ovalbumin encapsulation-enabled tandem reactive oxygen species generation, *Angew. Chem., Int. Ed.*, 2020, **59**, 20008–20016.

149 G. Li and Y. Zhang, Highly selective two-electron oxygen reduction to generate hydrogen peroxide using graphite felt modified with N-doped graphene in an electro-Fenton system, *New J. Chem.*, 2019, **43**, 12657–12667.

150 L. Lu, Q. Shu, G. Zhang, Q. Zhang, P. Du and X. Zhu, Mechanism in chlorine-enhanced Pd catalyst for H_2O_2 in situ synthesis in electro-Fenton system, *AIChE J.*, 2022, **68**, e17787.

151 D. Ozturk and M. Gulcan, Synthesis, characterization, and in-situ H_2O_2 generation activity of activated Carbon/Goethite/Fe_3O_4/ZnO for heterogeneous electro-Fenton degradation of organics from woolen textile wastewater, *J. Ind. Eng. Chem.*, 2023, **122**, 251–263.

152 A. Santos, R. J. Lewis, D. J. Morgan, T. E. Davies, E. Hampton, P. Gaskin and G. J. Hutchings, The oxidative

degradation of phenol via in situ H_2O_2 synthesis using Pd supported Fe-modified ZSM-5 catalysts, *Catal. Sci. Technol.*, 2022, **12**, 2943–2953.

153 M. Triki, S. Contreras and F. Medina, Pd–Fe/TiO_2 catalysts for phenol degradation with in situ generated H_2O_2, *J. Sol-Gel Sci. Technol.*, 2014, **71**, 96–101.

154 R. Underhill, R. J. Lewis, S. J. Freakley, M. Douthwaite, P. J. Miedziak, O. Akdim, J. K. Edwards and G. J. Hutchings, Oxidative degradation of phenol using in situ generated hydrogen peroxide combined with Fenton's process, *Johnson Matthey Technol. Rev.*, 2018, **62**, 417–425.

155 Y. Xing, Z. Yao, W. Li, W. Wu, X. Lu, J. Tian, Z. Li, H. Hu and M. Wu, Fe/Fe_3C boosts H_2O_2 utilization for methane conversion overwhelming O_2 generation, *Angew. Chem.*, 2021, **133**, 8971–8977.

156 Z. Yang, X. Zhang, S. Pu, R. Ni, Y. Lin and Y. Liu, Novel Fenton-like system (Mg/Fe-O_2) for degradation of 4-chlorophenol, *Environ. Pollut.*, 2019, **250**, 906–913.

157 R. Liu, Y. Chen, H. Yu, M. Polozij, Y. Guo, T. C. Sum, T. Heine and D. Jiang, Linkage-engineered donor-acceptor covalent organic frameworks for optimal photosynthesis of hydrogen peroxide from water and air, *Nat. Catal.*, 2024, **01102**, 3.

158 J. Li, J. Zhang, Y. Wang, H. Wang and H. Song, Preparation of highly active g-C_3N_4 supported amphiphilic quaternary ammonium phosphotungstate catalyst for solvent-free oxidative desulfurization of benzothiophene, *React. Kinet., Mech. Catal.*, 2022, **135**, 219–231.

159 X. Yu, P. Han and Y. Li, Oxidative desulfurization of dibenzothiophene catalyzed by α-MnO_2 nanosheets on palygorskite using hydrogen peroxide as oxidant, *RSC Adv.*, 2018, **8**, 17938–17943.

160 P. T. Cherop, S. L. Kiambi and P. Musonge, Modelling and optimisation of oxidative desulphurisation of tyre-derived oil via central composite design approach, *Green Process. Synth.*, 2019, **8**, 451–463.

161 C. G. Piscopo, J. Tochtermann, M. Schwarzer, D. Boskovic, R. Maggi, G. Maestri and S. Loebbecke, Titania supported on silica as an efficient catalyst for deep oxidative desulfurization of a model fuel with exceptionally diluted H_2O_2, *React. Chem. Eng.*, 2018, **3**, 13–16.

162 V. Tamborrino, G. Costamagna, M. Bartoli, M. Rovere, P. Jagdale, L. Lavagna, M. Ginepro and A. Tagliaferro, Catalytic oxidative desulphurization of pyrolytic oils to fuels over different waste derived carbon-based catalysts, *Fuel*, 2021, **296**, 120693.

163 L. Wang, Z. Li, G. Jin, N. Zuo and Y. Xu, Effort of ionic liquids with $[HSO_4]^-$ on oxidative desulphurization of coal, *Can. J. Chem. Eng.*, 2019, **97**, 1299–1306.

164 X. Li, J. Zhang, F. Zhou, Y. Wang, X. Yuan and H. Wang, Oxidative desulfurization of dibenzothiophene and diesel by hydrogen peroxide: Catalysis of $H_3PMo_{12}O_{40}$ immobilized on the ionic liquid modified SiO_2, *Mol. Catal.*, 2018, **452**, 93–99.

165 D. Xie, Q. He, Y. Su, T. Wang, R. Xu and B. Hu, Oxidative desulfurization of dibenzothiophene catalyzed by peroxotungstate on functionalized MCM-41 materials using hydrogen peroxide as oxidant, *Chin. J. Catal.*, 2015, **36**, 1205–1213.

166 H. Guo, L. Zhou, K. Huang, Y. Li, W. Hou, H. Liao, C. Lian, S. Yang, D. Wu, Z. Lei, Z. Liu and L. Wang, Nitrogen-rich carbon dot-mediated n→π electronic transition in carbon nitride for superior photocatalytic hydrogen peroxide production, *Adv. Funct. Mater.*, 2024, **34**, 02650.

167 H.-X. Qi, S.-R. Zhai, W. Zhang, B. Zhai and Q. D. An, Recyclable HPW/PEHA/ZrSBA-15 toward efficient oxidative desulfurization of DBT with hydrogen peroxide, *Catal. Commun.*, 2015, **72**, 53–56.

168 S. Liang, K. Hofman, M. Friedrich, J. Keller and G. Manolikakes, Recent progress and emerging technologies towards a sustainable synthesis of sulfones, *ChemSusChem*, 2021, **14**, 4878–4902.

169 W. Wu, Y. Bai, X. Wang and C. Wu, Sulfone-based high-voltage electrolytes for high energy density rechargeable lithium batteries: Progress and perspective, *Chin. Chem. Lett.*, 2021, **32**, 1309–1315.

170 R. Trivedi and P. Lalitha, VCl_3-catalyzed selective oxidation of sulfides to sulfoxides using H_2O_2 as oxidant, *Synth. Commun.*, 2006, **36**, 3777–3782.

171 S. L. Jain and B. Sain, Perfluorinated resinsulphonic acid (Nafion-H®) catalyzed highly efficient oxidations of organic compounds with hydrogen peroxide, *Appl. Catal., A*, 2006, **301**, 259–264.

172 J. Přech, R. E. Morris and J. Čejka, Selective oxidation of bulky organic sulphides over layered titanosilicate catalysts, *Catal. Sci. Technol.*, 2016, **6**, 2775–2786.

173 K. Bahrami and M. Khodamorady, Reusable BNPs-SiO_2@$(CH_2)_3NHSO_3H$-catalysed selective oxidation of sulfides to sulfones, *Appl. Organomet. Chem.*, 2018, **32**, e4553.